Olfactory information processing in a Parkinson's disease mouse model

A Thesis Submitted to

Indian Institute of Science Education and Research Pune

in partial fulllment of the requirements for the

BS-MS Dual Degree Programme by

Kaushik Shailesh More

Registration Number: 20141137

IISER PUNE

Indian Institute of Science Education and Research Pune

Dr. Homi Bhabha Road,

Pashan, Pune 411008, India.

March, 2019

Supervisor: Dr. Nixon M. Abraham

Certificate

This is to certify that this dissertation entitled **"Olfactory information processing in a Parkinson's disease mouse model"** towards the partial fulllment of the BS-MS dual degree programme at the Indian Institute of Science Education and Research, Pune represents study/work carried out by Kaushik More at Indian Institute of Science Education and Research, Pune under the supervision of Dr. Nixon M. Abraham, Assistant Professor, Department of Biology, during the academic year 2018-2019.

Kaushik More   Dr. Nixon M. Abraham

Declaration

I hereby declare that the matter embodied in the report entitled **"Olfactory Information processing in a Parkinson' Disease mouse model"** are the results of the work carried out by me at the Department of Biology, Indian Institute of Science Education and Research, Pune, under the supervision of Dr. Nixon M. Abraham and the same has not been submitted elsewhere for any other degree.

Kaushik More   Dr. Nixon M. Abraham

Abstract

Olfactory dysfunction is one of the earliest clinical symptoms of Parkinson's disease (PD), preceding the onset of the motor deficits. PD occurs as a result of altered α-synuclein (α-syn) expression leading to its aggregation. α-syn is a natively unfolded protein found in various bodily tissues. In brain, it is predominantly found in the pre-synaptic terminals where they are involved in vesicular transport. α-syn aggregates can be found in Lewy bodies and Lewy neurites in neural tissues, which are a characteristic pathophysiological hallmarks of PD. In this project, we created a PD mouse model by injecting the abnormally aggregated forms of human wild type α-syn into the olfactory bulb of wild type mice. A series of olfactory behavioral assays were carried out to check for any sensory impairment. Their olfactory behavior was studied in detail by analyzing the detection and discrimination abilities of mice using a go/no-go operant conditioning paradigm. Mice injected with oligomeric and fibrillar forms of α-syn exhibited impaired learning and longer reaction times for the first complex odor pair discrimination that we performed. The learning improved when a subsequent odor discrimination task was done. However, they still showed the reaction time phenotype. We also investigated if our strategy led to the development of characteristic motor impairments or anxiety-like behaviors in our mouse model. As these mice did not exhibit any motor deficits, they offer as an ideal model to study the physiological basis of smell dysfunction observed in PD patients.

List of figures

List of tables

Table of Contents

Acknowledgments

1. Introduction

Neurodegenerative diseases can be defined as diseases involving a progressive loss in the structural integrity and functionality of neurons, which may lead to cell death. Parkinson's, Alzheimer's, Huntington's, etc are commonly observed in adult patients. The nervous system is responsible for coordinating the crosstalk and functions of different organs in the body. Neurons can be considered as the most basic building blocks of the nervous system. In neurodegenerative diseases, the health and diverse population of excitatory & inhibitory neurons are severely affected. Therefore, the neuronal cytotoxicity caused due to neurodegenerative disease is very unlikely to be reversed or cured, thus affecting the quality of life significantly (Lee and Trojanowski, 2006; Welsh, 2001). We can delay the progression of such neurodegenerative diseases, but a permanent cure has not been found for any of these neurodegenerative diseases. These neurodegenerative diseases are becoming increasingly prevalent in a significant fraction of the elderly human population (Heemels, 2016, Neurological disorders: Public health challenges (WHO report), 2007).

The olfactory system plays a pivotal role in the detection of chemical signals in the environment of animals. The olfactory system is regarded as the primary sensory modality involved in chemosensation (Lledo et al., 2005). Animals employ their olfactory system to accomplish a wide array of tasks such as locating their food/prey, evading from their predators, to find conspecifics and mates, etc. The olfactory system is responsible for odor detection, discrimination and processing thus affecting the decision-making behaviors of the organism.

1.1 Neurodegeneration and olfactory system

The pathophysiology of neurodegenerative diseases is vast, ranging from affecting an individual's cognitive abilities to causing sensory and motor impairments amongst the affected. One such specific impairment includes the olfactory perceptual deficits, which is seen across a large number of individuals who are affected with neurodegenerative diseases. Impairment in olfaction may indicate difficulties in odor identification, odor detection, odor discrimination and odor memory (reviewed in Rey et al., 2018b).

Olfactory deficits are observed earlier as compared to the major motor and cognitive symptoms across these neurodegenerative diseases, thus also being called as a prodromal symptom of these diseases (Adler, 2011; Hüttenbrink et al., 2013). Given the fact, that the olfactory epithelium is in contact with the external environment, it becomes an access point for the entry of pathogens and toxins into the brain. This entry of toxic foreign entities may lead to a chain of pathological changes across the brain thus affecting various regions of the brain (Doty, 2008; Hobson, 2012). The native endogenous proteins of the individual are affected by these external agents entering through the olfactory tract leading to misfolding and aggregation, which are resistant to breakdown by the innate defense mechanisms of the body. These abnormally aggregated forms of proteins can further spread to the various regions of the brain as described in the prion ("proteinaceous infectious particles") hypothesis, according to which, the abnormal, misfolded proteins can act as seeds for aggregation of the normal protein thus initiating a self-propagating chain reaction for the progression of the disease (Jucker and Walker, 2013; Kordower et al., 2011; Prusiner, 2001; Rey et al., 2013).

Parkinson's disease (PD) ranks second to Alzheimer's disease (AD) as the most common neurodegenerative disease (Meissner et al., 2011) and is characterized by the selective cytotoxicity of dopaminergic neurons in the substantia nigra pars compacta (SNpc) region of the brain. The presence of Lewy bodies and Lewy neurites in the affected regions of the brain are a classical hallmark of PD (Braak et al., 2003; Wakabayashi et al., 2007). Deficits in the olfactory abilities of patients affected with PD were first reported as early as in 1975 by Ansari and Johnson. Impairment in olfactory

abilities is seen as an early symptom of PD, manifesting themselves as early as four years before the appearance of the motor symptoms associated with the disease (Ponsen et al., 2004; Ross et al., 2008). Braak and coworkers have suggested that the pathophysiology of PD generally initiates in the olfactory bulb and/or anterior olfactory nucleus, the enteric nervous system and the dorsal motor nucleus of the vagus nerve (DMX) (Braak et al., 2003).

1.2 α-synuclein and its role in Parkinson's disease

α-synuclein (α-syn) is a protein encoded by the SNCA gene in humans involved in vesicular release and trafficking across synapses, thus mainly present at the presynaptic terminals of the neurons(Diao et al., 2013) . In its wild type form, α-syn is comprised of 140 residues, divided amongst three different domains, the N-terminal domain (amino acid 1-65), a non-amyloid-β component of plaque (NAC) domain (amino acid 66-95) and a C-terminal domain (amino acid 69-140)(reviewed in Emamzadeh, 2016; Stefanis, 2012). It is present in an intrinsically disordered structure as indicated by spectroscopic studies and found in abundance throughout the brain (Fink, 2006). This is mainly due to the high net negative charge of the protein at a neutral pH and its low intrinsic hydrophobicity (Uversky et al., 2000). The presence of cytoplasmic or intercellular α-syn in its abnormally aggregated form is a characteristic of PD. These aggregated forms of α-syn are a major component of the Lewy bodies and Lewy neurites (Figure 1)(Lee and Trojanowski, 2006). The aggregation of α-syn is believed to be a critical step in the onset of PD. The early onset of PD is characterized by either the presence of six different missense mutations in the α-syn coding gene (SNCA gene) or the over-expression of wild type α-syn protein which is caused due to gene triplication (Dehay et al., 2015; Flagmeier et al., 2016; Singleton et al., 2004, 2003).

The fibrillation of α-syn is a nucleation-dependent process (Wood et al., 1999), which means aggregated α-syn molecules can act as seeds to initiate nucleation of the monomeric wild-type endogenous α-syn, thus spreading the pathology across different regions of the brain (Rey et al., 2018b). There are competing kinetic pathways for the aggregation of α-syn. A natively unfolded monomeric protein gets converted to a partially folded intermediate which can get converted to different aggregated forms like amorphous aggregates or oligomers or fibrils depending on the concentration of the protein and aggregation conditions (Fink, 2006).

In vitro and *in vivo* studies have been conducted to show the transfer of α-syn from one cell to another, thus proving the seeding hypothesis of propagation of aggregated α-syn from the affected cell to neighboring cells (Angot et al., 2012; Danzer et al., 2009; Luk et al., 2009). The α-syn pathology is seen in the mitral cells, tufted cells (principal projection neurons), the periglomerular cells and the granule cells (inter-neurons) of the olfactory bulb (Sengoku et al., 2008). As the mitral cells and tufted cells are projection neurons, the downstream olfactory cortical areas also receive significant amount of Lewy bodies and Lewy neurites as the disease progresses(Rey et al., 2016).
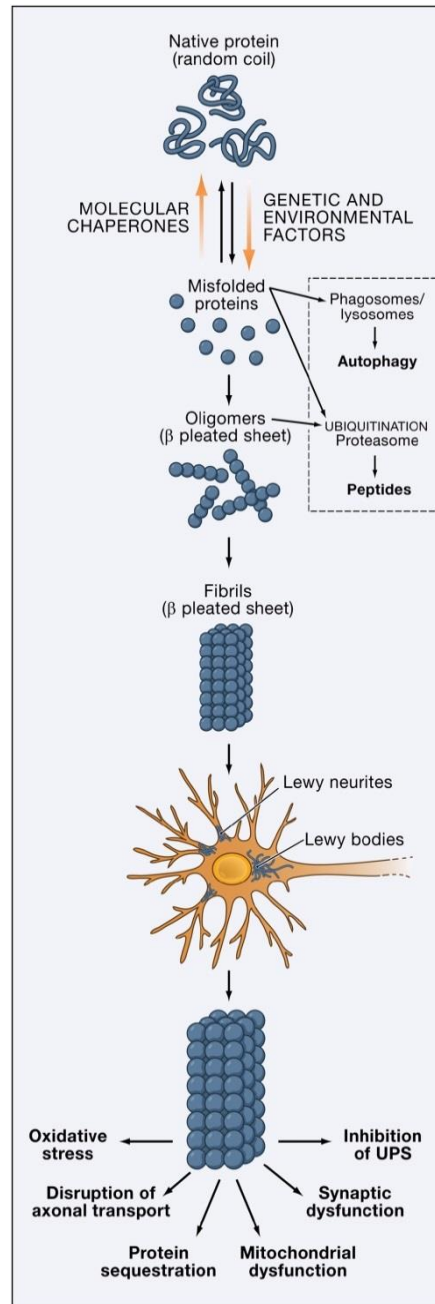
Figure 1: A model of aggregation of α-synuclein and downstream effects (Lee and Trojanowski, 2006)

1.3 The sense of smell in Parkinson's disease rodent models

The olfactory system is one of the prime sensory systems which are used by rodents to interact with their environment. They use it for foraging, detection of mates and predators, and other social behaviors. The olfactory system in rodents is subdivided into three major parts: the periphery, the olfactory bulb (OB), and the olfactory cortex (Figure 2) (Lledo et al., 2005). In the nose, the odorant receptors (OR) present on olfactory sensory neurons (OSN) in the olfactory epithelium detect the odor molecules. These ORs belong to a family of G-Protein Coupled Receptors (GPCRs) which activate downstream signal transduction finally resulting in an action potential. (Buck and Axel, 1991; Mombaerts, 2001). The olfactory system employs a combinatorial approach of ORs to recognize different odors. This means that instead of just an individual OR recognizing a particular odor, the olfactory system detects odors by different combinations of the ORs (Malnic et al., 1999). The MOB is made up of five different cell layers:

- Glomerular layer (GL)
- External plexiform layer (EPL)
- Mitral cell layer (MCL)
- Internal plexiform layer (IPL)
- Granule cell layer (GCL) (Shepherd, 2004)

The GL receives sensory inputs from the olfactory sensory neurons. As the name suggests, this layer is made up of a number of neuropil-like structures called glomeruli where the axons from the OSNs terminate. The arrangement of these glomeruli is such that a particular glomerulus receives the inputs from the olfactory sensory neurons which express the same odorant receptor (Mombaerts et al., 1996; Ressler et al., 1993). Thus, a spatial map of different odors is made in this layer. The periglomerular (PG) cells, external tufted (ET) cells and the superficial short-axon (sSA) cells are the three distinct cell types which are surrounding the glomeruli in the GL which are collectively called as juxtaglomerular (JG) cells (reviewed in Nagayama et al., 2014). The MCL

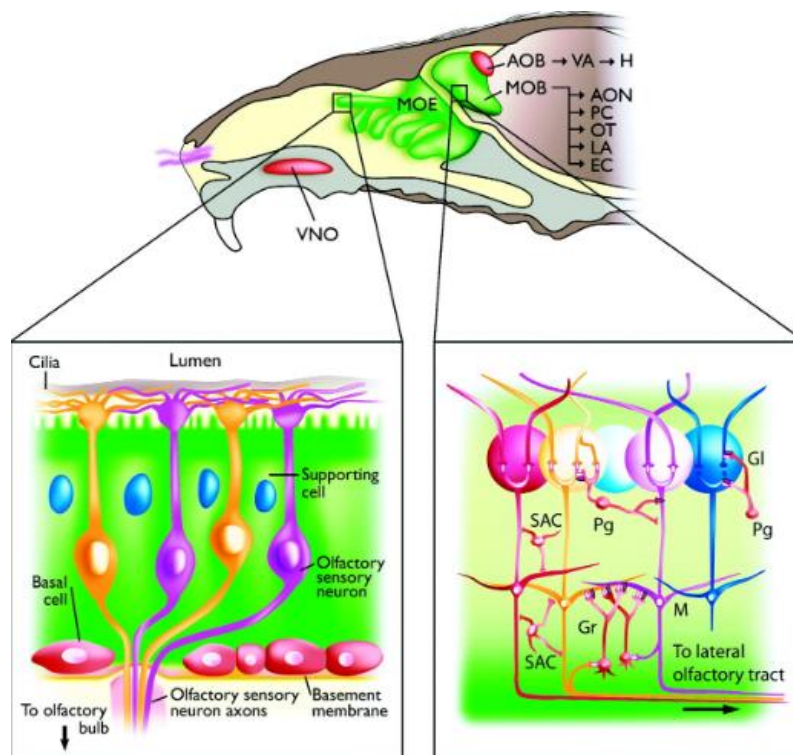Figure 2: A diagrammatic representation of the rodent olfactory system. (From Lledo et al., 2005). Sagittal section of the rodent brain is depicted in the top diagram. The lower left diagram is a representation of the olfactory epithelium depicting olfactory sensory neurons. The lower right diagram is the representation of the connections in the main olfactory bulb.

contains the somata of mitral cells and tufted cells, which are the projection neurons that carry information to higher brain centers. Excitatory glutamatergic synapses are formed between the afferent axons of the OSNs and the apical dendrites of mitral and tufted (M/T) cells in the glomeruli. GCL is primarily made up of interneurons called granule cells (GC) (Price and Powell, 1970). These cells are axon-less, and their primary function is to provide recurrent and lateral inhibition to mitral and tufted cells. They receive excitatory glutamatergic inputs from the mitral and tufted cells, which leads to a GABA release from their spines. If the GABA is released to the same mitral cells which had excited the GC, the process is known as recurrent inhibition while if it is released onto the dendrites of neighboring mitral cells, it is called lateral inhibition (Isaacson and Strowbridge, 1998; Margrie et al., 2001; reviewed in Shepherd et al., 2007). The inhibition provided by the interneurons to the projection neurons is highly activity-dependent. Because of this, the spatio-temporal representation for each odor is unique, although, it can be overlapping for perceptually similar odors. Such dense bi-directional connectivity, thus, plays an important role for odor contrast enhancement. This makes OB as the first centre where odor perception can be partially achieved. The mitral and tufted cells further project to the olfactory cortex, which includes the anterior olfactory nucleus (AON), the piriform cortex (PC), the olfactory tubercle (OT), the lateral part of the cortical amygdala (LA), and the entorhinal cortex (EC).

There have been studies in which different forms of α-syn (human wild type, human oligomeric, human and mice pre-formed fibrils (PFFs), and human fibrils) have been injected in the olfactory bulb of mice to study their spread and effect on cell population (Rey et al., 2013, 2016, 2018b). One of the studies (Rey et al., 2013) showed that the human α-syn (monomeric, oligomeric and fibrillar) which was injected in the olfactory bulb of the mice was capable of transferring to the interconnected brain regions. The injection of mouse PFFs as well as human PFFs into the OB of mice is capable of causing the spread of α-syn pathology to the interconnected regions of the brain although the progression in case of human PFFs being comparatively slower than that of mice PFFs. They also showed that this spread of the α-syn pathology after the injections of α-syn PFFs is associated with an increased neuronal cell loss in the OB

over a time period of 6-months post injection. However, the pathology was observed to decrease in its severity at a time point of 18 months in their model(Rey et al., 2018b).

1.4 Our Work

We have developed a Parkinson's disease mouse model to check for any olfactory impairments caused by the injection of aggregated forms of α-syn in the olfactory bulb of wild type mice. Three groups of wild type mice were stereotactically injected with structurally different forms of human α-syn i.e. monomeric, oligomeric and fibrillar forms in the granule cell layer (GCL) of the olfactory bulb, respectively. An array of sensory and motor behavioral experiments were then performed. Granule cells play an essential role in lateral and recurrent inhibition of mitral/tufted cells, which is pivotal in odor discrimination(Abraham et al., 2004, 2010; Bhalla and Bower, 1993; Johnson et al., 2010). The main hypothesis behind this study is that the injection of α-syn in the GCL would lead to the development of PD pathology as a result of dysfunction in the inhibitory interneuronal synaptic connections. This would, in turn, affect the odor detection & discrimination abilities of the animals. The olfactory learning, long-term memory and reaction times are the parameters investigated in these injected mice using a go/no-go operant conditioning paradigm (Abraham et al., 2004, 2010). We also carried out a series of non-associative olfactory behavioral assays such as pheromone detection assay and the buried food pellet test. To check whether our injections had any effect on the accessory olfactory bulb mediated behavior such as pheromone detection, a pheromone detection test was carried out (Bind et al., 2013). The buried food-pellet test was performed to check for odor detection abilities of the injected mice (Machado et al., 2018). Regular administration of α-syn aggregates through nose in adult mice for 14 days led to rigidity and locomotor defects (Gruden et al., 2014).In order to investigate if our intrabulbar injections α-syn led to any motor dysfunction we carried out the vertical pole test (Ogawa et al., 1985). Pre-motor symptoms include not only olfactory dysfunctions but also elevated anxiety levels (reviewed in Prediger et al., 2012). Thus we carried out the open-field test to check if our PD models exhibited increased anxiety and exploratory activity (Takahashi et al., 2006).

2. Materials and Methods

2.1 Subjects

A total of 27 C57BL6J male mice were obtained from the National Facility for Gene Function in Health and Disease, IISER Pune. The subjects were of age around 6-8 weeks during the beginning of stereotactic injections. The 27 subjects were divided into 3 groups of 9 animals each. Each group was further subdivided amongst two sets wherein one set contained 4 animals while the other set housed 5 animals. The animals were maintained on a 12-hour light and 12-hour dark cycle in cages under humidity and temperature controlled conditions. The subjects had free access to food during the training period, but were kept on a 12-hour water deprivation cycle such that they maintained ≥80% of their baseline body weight. The procedures were approved by the Institutional Animal Ethics Committee (IAEC) and Committee for the purpose of Control and Supervision of Experiments on Animals (CPCSEA), Govt. of India.

2.2 Odors

The odors used were Nonanol (Nn),1-Heptanol(Hp), (S)-(+)- Octanol (+O) and (R)-(-)-Octanol (-O). Odors were diluted in 1 % mineral oil. Complex mixtures of these odors were made in a ratio of 60:40. The first odor pair was Hp vs. Nn and the second odor pair was +O vs. –O.

2.3 Three structural forms of α-synuclein

We injected three structurally different forms of human α-synuclein into three groups of animals. The protein purification and aggregates preparations were carried out by Lisni P. Sunny, a student in our lab. The protein was expressed in BL21 (DE3) *E. coli* bacteria and purified by anion exchange chromatography. The stock protein of

concentration 100 μM was kept for aggregation in PBS (pH 7.4) in a thermomixer at 37 °C and 600 r.p.m and characterized by transmission electron microscopy to check for the aggregated forms of the protein (Figure. 3). A stock protein of concentration of 70 μM was incubated under the same conditions, and atomic force microscopy was done to check for the oligomeric form of the protein (Figure. 4). The stock protein which was not subjected to the treatment above mentioned was used as monomeric form of the protein.
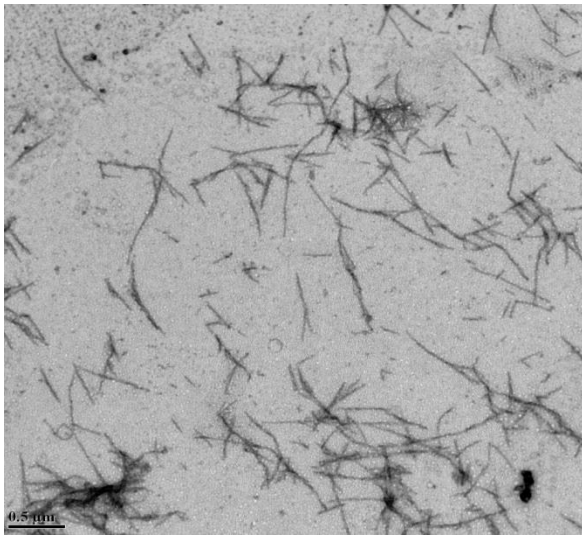
Figure 3: TEM image showing α-synuclein fibrils (Scale 0.5 μm)
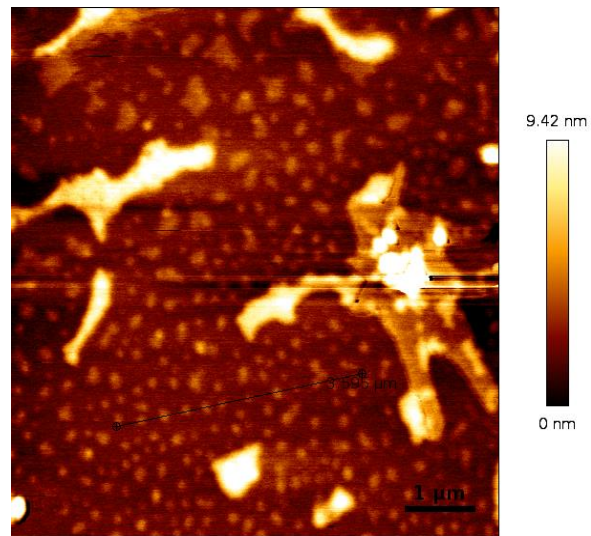
Figure 4: AFM image showing α-synuclein oligomers (Scale 1 μm)

2.4 Stereotaxic Surgeries

Three different groups of wild type mice were stereotactically injected with three different structural forms of α-syn as follows:

Group 1: Monomers injected mice

Group 2: Oligomers injected mice

Group 3: Fibrils injected mice

The animals were anesthetized using a Ketamine:Xylazine mixture which was administered intraperitoneally. The amount of ketamine used was 60 mg/ml/kg body weight of animal and xylazine was 10 mg/ml/kg body weight of the animal. After anesthetizing, the animals were mounted on the stereotaxic setup (Figure.5) (Leica Angle Two Stereotaxic-220V for Mouse). The head of the animal was held in place using two ear bars. The upper jaw was fixed on a tooth-ring.

Manipulators for adjusting the AP, ML and DV axes

Tooth ring

Ear Bars
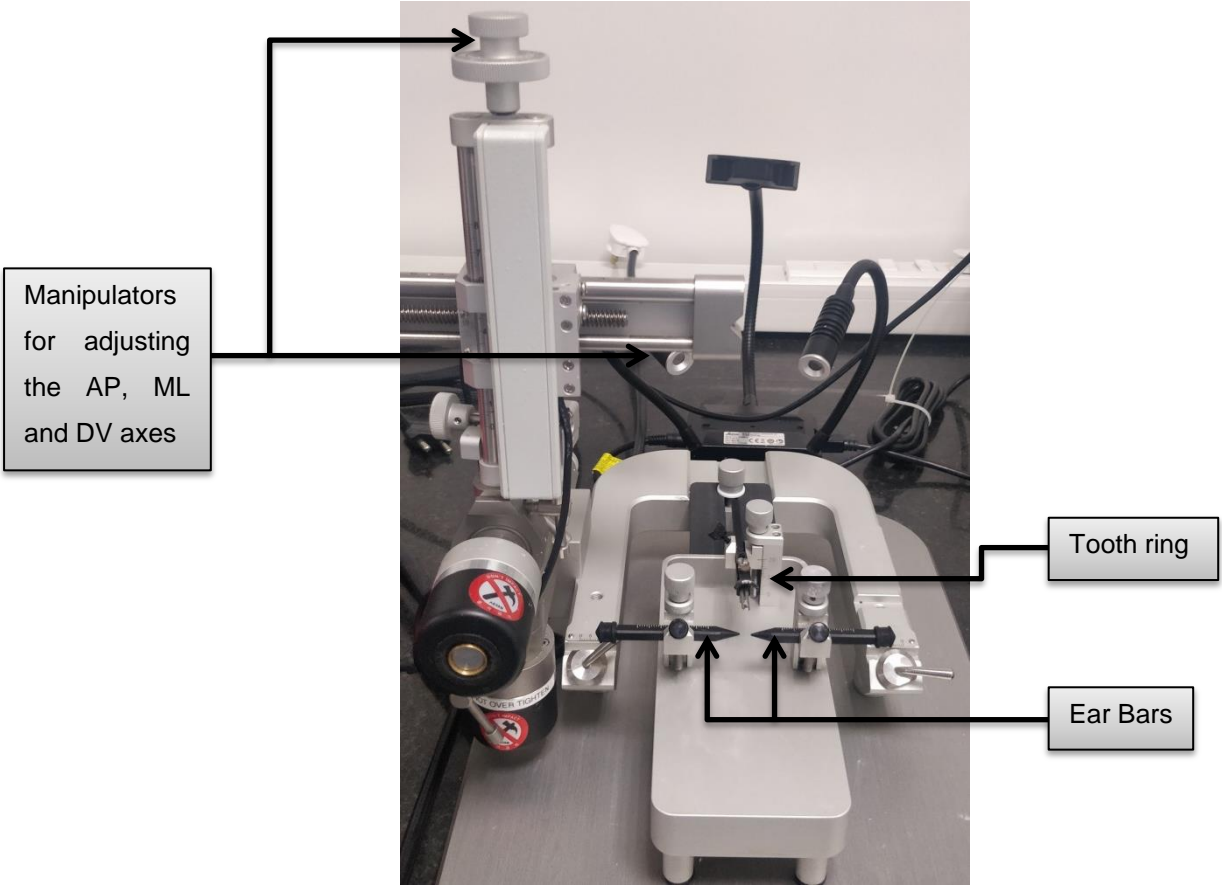
Figure 5: Stereotaxic setup

After mounting, the hair was shaved off to expose the skin. Using a scalpel blade, a straight cut (approx. 2 cm) was made in the skin directly above the skull. The skin was retracted to form a lateral window for craniotomy and held in place with the hooks. The area was cleaned and kept moist with cortex buffer (1x). A craniotomy was then performed using a Bien Air Black Pearl Eco turbine.
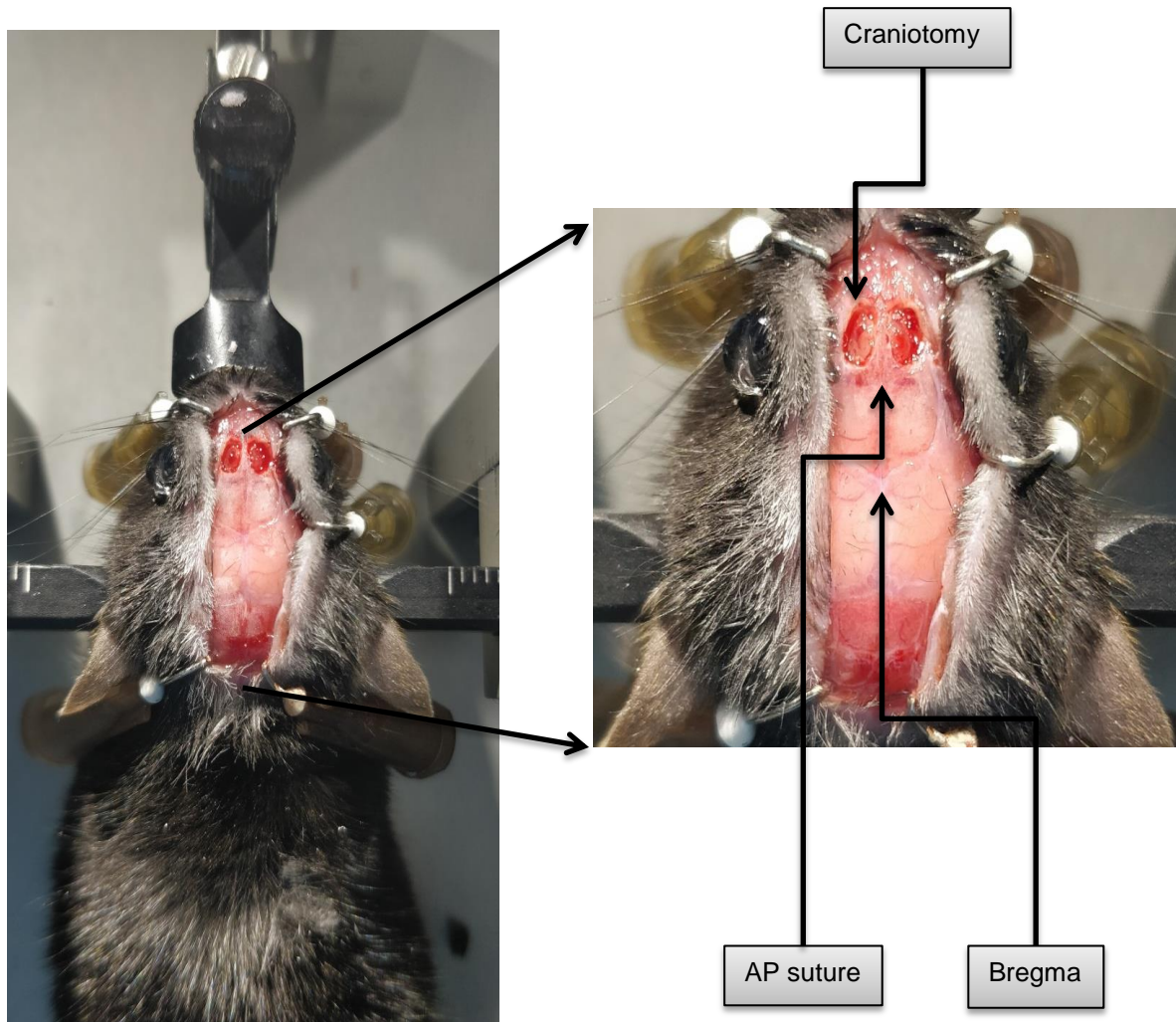
Figure 6: Images of craniotomy performed on a wild type mouse to inject the aggregated forms of α-synuclein

Two cranial windows of approximately 2.5 mms in length were drilled, one above each olfactory bulb, as shown in the figure (Figure. 6).

Blaubrand micropipettes (5µl), which were pulled on Narishige Japan horizontal puller (model PN-31), were used to make the injection capillaries. The plane between the bregma and the antero-posterior suture (AP suture) was made parallel by adjusting the height of the tooth ring. These adjustments were done because the stereotactic injection coordinates were defined relative to the center of OB on the dorsal side. The injection capillary was then positioned to the center of the bulb on one side and the x, y and z coordinates were set to zero. Protein of concentration 1mg/ml was then loaded in the injection capillary. With respect to the center point, four injections were made in the granule cell layer of the OB at co-ordinates defined in (Abraham et al., 2010). The co-ordinates were as follows: (0.5, 0, -1), (0.3, 0,-1.3), (0.1, 0, -1.4) and (0.1, 0, -2) all in mms along the (AP, ML, DV) axes. 0.4 µl of 1 mg/ml protein was injected at one site and then the capillary was held in place for 4 mins to ensure proper delivery of protein. After 4 minutes the capillary was retracted and adjusted to the other sites for further injections. After the injections in one bulb were carried out, the center point for the other bulb was adjusted in the same way, and the injections were carried out in the other bulb.

Thus, a total of 8 injections per animal were carried out with 0.4 µl of 1 mg/ml protein injected at each site, i.e. a total of 3.2 µl of 1 mg/ml protein was injected per animal. After the injections, the hooks were removed, and skin was retracted. The incision was sutured up, and the mouse was kept on a heating pad until waking up from anesthesia.

2.5 Behavioral training

The behavioral training was carried out after a recovery period of two weeks after the stereotaxic surgeries.

2.5.1 Go/no-go paradigm

The odor discrimination abilities of mice were examined by training the animals on a task based on go/no-go operant conditioning paradigm, to distinguish between binary

mixtures of odors (Abraham et al., 2004). All experiments were done using the custom-made eight channel olfactometers. Mouse was kept in an operant chamber where it had access to a sampling tube guarded by an infrared (IR) beam. When the mouse breaks the beam and enters the sampling tube, the trial is initiated. Upon the initiation of a trial, the mouse is presented with an odor, which can be either the rewarded odor (S+) or the non-rewarded odor (S-). The odor and final (diversion) valves controlled the flow of odor in a time-dependent manner, allowing opening of final valve 500ms after odor valve opening. Each time, a particular odor was presented through either of the two valves. A total of four odor valves for two odors (rewarded and unrewarded) were used.

The animal has to lick on the water delivery tube for the S+ odor and retract its head from the sampling tube in case of S- odor. The animal does not receive any punishment if it licks for the S- odor (Figure. 7)
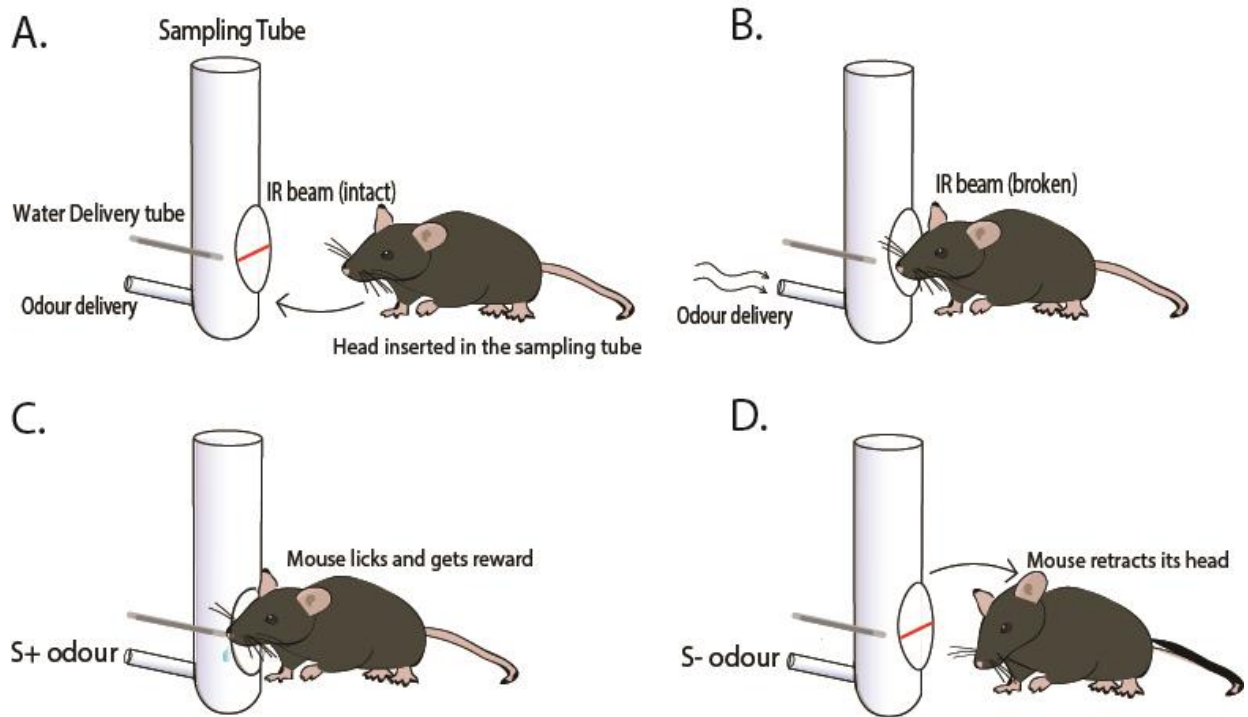

Figure 7. Go/no-go paradigm. **A**. The mouse has to break the IR beam to initiate the trial. **B**. Once the IR beam is broken an odor is delivered to the mouse. **C**. If it is a rewarded (S+) odor, the mouse has to lick on the water delivery tube for required time and it gets a water reward. **D**. If it is non-rewarded (S-) odor, the mouse retracts its head and the IR beam is resealed.

2.5.2 Reward Criterion

The total stimulus duration of 2s was divided into 4 bins of 500ms each. When a rewarded odor (S+) is presented, the mouse has to lick at least once in 3 out of 4 bins to register a successful trial after which it receives a water reward of 3-4µl. If a non-rewarded odor (S-) is presented, the mouse should not lick for more than 2 bins out of 4 to register a successful trial. During the presentation of S+ odor, if the animal does not lick for at least 3 bins out of 4 then the trial gets registered as an unsuccessful trial. In case of S- trial if the animals licks for more than 2 bins, then the trial gets registered as an unsuccessful trial.

2.5.3 Apparatus

The odor discrimination experiments were done on three different custom-built Knosys eight-channel olfactometers (Bodyak and Slotnick, 1999). The software used for controlling the olfactometers was custom written in Igor, Wavemetrics (Abraham et al., 2004).

The animal was kept in an operant chamber consisting of a small circular opening into the sampling tube, which is 2.5cm in diameter. The opening was guarded by an IR beam and a photodiode receiver. When the animal pokes its head into the sampling tube and breaks the beam, the trial is initiated. Upon initiation of the trial, the animals receive one of the two (S+ and S-) odors from the valves (2 valves each) and have to make the decision accordingly. Figure 8 shows the olfactometer setup.
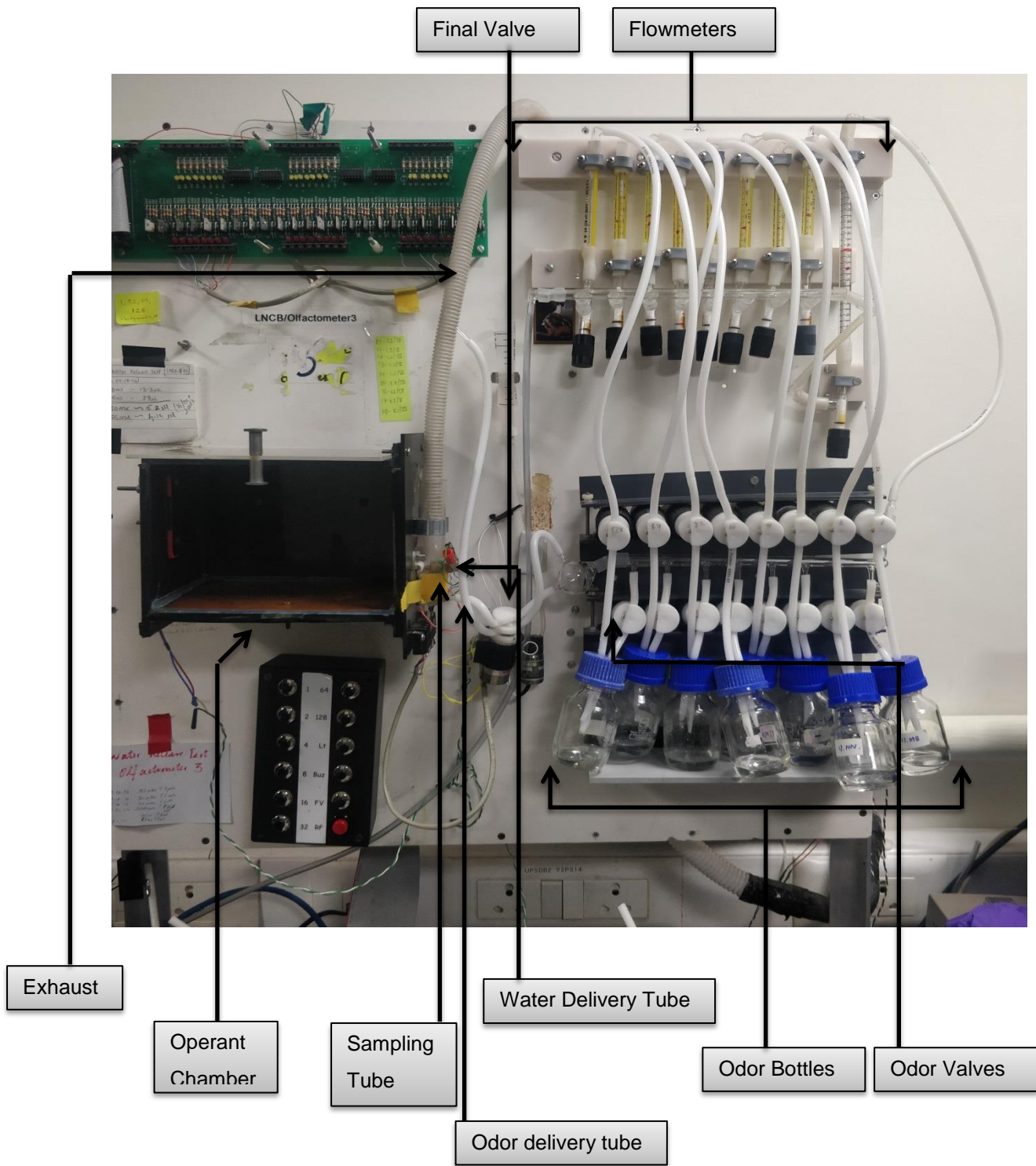
Figure 8: Olfactometer setup

2.5.4 Pre-training

The mice that were at ≥80% of their baseline body weight after 2-3 days of 12-hour water deprivation schedule underwent a pre-training task to get the animal acquainted with the design of the setup, the sampling tube, and the water delivery tube. The pre-training task is divided into 9 phases. Phase 0 contains 5 trials wherein the mouse gets the reward by poking its head in the sampling tube. It helps the mouse to know the location of the water delivery tube. In phase 1 (15 trials), the animal needs to lick on the water-delivery tube to get the reward. From phase 2 onwards till phase 8, there are 20 trials per phase for which the animal has to lick the on the water delivery tube after odor presentation to receive a reward. The odor used here is that of the mineral oil in which our odor dilutions are prepared. The duration for which the animal has to lick gradually increases as the phases progress, with the reward criteria becoming identical to that of the training protocol in the last two phases.

2.5.5 Olfactory discrimination training

In the odor discrimination task, the trial is initiated when the mouse breaks the IR beam guarding the sampling tube. This leads to opening of a diversion valve (Dv) and one of the four main odor valves. The Dv is responsible for optimizing the odor traveling time between its onset and first contact with the animal. When the Dv is released, odor is applied to the animal for a total duration of 2 seconds. Odors are presented to the animal in a pseudorandomized manner such that in a block of 20 trials not more than two consecutive trials are of the same odor. Each block had 10 rewarded (S+) and 10 non-rewarded (S-) trials. There was a minimum inter-trial interval (ITI) of 5 seconds between the end of one trial and the resealing of the IR beam for the next trial. Three tasks of 300 trials were carried out for both the odor pairs.

2.5.6 Olfactory behavior task readouts

The **percentage accuracy** of an animal for an olfactory discrimination task is defined as the percentage of successful trials the animal performs in the task. **Learning curves** for different odor pairs was plotted as a measure of percentage accuracies at regular intervals of 100 trials. Initial learning occurs at chance level as the mouse is unaware as to which of the two odors is unrewarded. Thus, it continues to lick equally well for both the S+ and S- odors. Upon training, after a few hundred trials, mouse learns to discriminate. A mouse finally achieves an accuracy of 90-95% at about 800-1200 trials. Learning, thus, is dependent on the complexity of the odors presented to the animals. Quicker learning is achieved in case of a task wherein mouse discriminates monomolecular odorants.

The **sample pattern** gives us an estimate about the time a mouse is spending in response to a rewarded or an unrewarded odor during training. Initially, the mouse will continuously break the beam and sample both the S+ and S- odors. However, over the training phase, mouse will start to retract its head for S- odors. Therefore, the sampling between the two odors would yield a sigmoidal curve. **Reaction time**, is, thus calculated from the sample pattern plotted for an average of 300 trials, as the time point after odor onset at which the pattern for S+ and S- diverges. The statistical difference between the two curves is plotted as a logarithmic graph and the last time point corresponding to p-value <0.05 is considered as the reaction time.

Lick percentage gives us a measure of the time spent by a mouse licking onto the lick tube during the stimulus duration of 2s. Initially, mouse licks for both the S+ and S- odors yielding a value of 80-90% in the initial training phase. However, as the mouse learns to discriminate, this value goes down to 50%, i.e the mouse licks only for 50% of the trials when the S+ odor is presented. **Inter-trial interval** or ITI is the time between two consecutive trials. It is calculated from the breaking of the IR beams at the beginning of the two consecutive trials. The lick percent as well as the ITI are an indirect measure of an animal's motivation. If the animal is motivated, then the ITI would be low as the animal will perform the trials quickly. Conversely, if the animal is not motivated,

the time between two consecutive trials would be more and lick percent would be below 50%.

2.6 Analysis

The data were analyzed using custom made software written in Igor (Abraham et al., 2004) for the above parameters and plotted using GraphPad Prism software.

2.7 Vertical pole test

The Vertical pole test (Ogawa et al., 1985) is a behavior test which is used to assess the motor dysfunction in animals. The mice are placed at the top of a vertical pole (Figure 9) of 50 cm height and diameter of 1 cm. The mice are kept snout up, top on the pole. The time taken to make a completely downward turn of the snout (T turn) and the total time taken to descend the pole (T total) are measured. Three trials were taken per animal, and then the average T turn and T total values were used for data analysis.

50 cm long pole
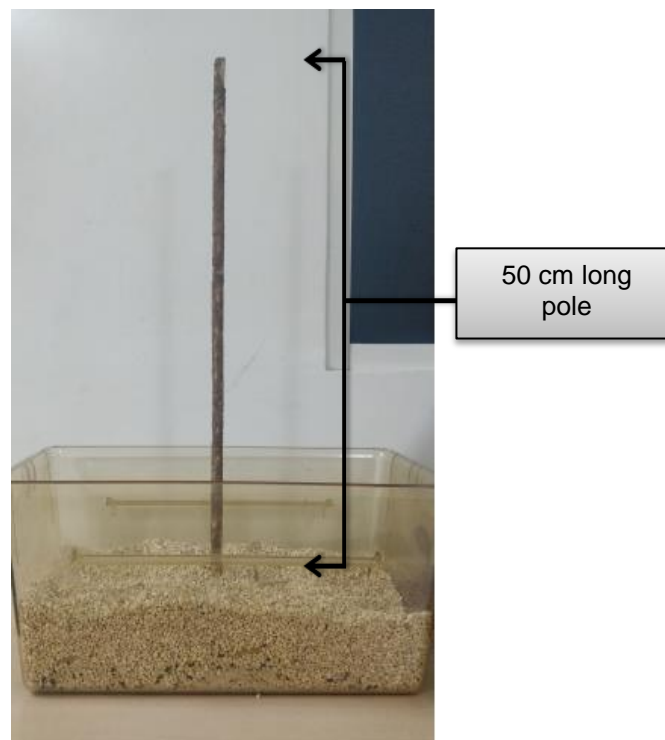
Figure 9: Pole test setup

2.8 Open Field Test

The open field test (OFT) was carried out to check the anxiety levels and general locomotive activity across the three groups. Individual mice were let into a rectangular arena of dimension 60 cm*45 cm*43 cm (length*breadth*height) (Figure. 10) for a time period of 10 minutes. The parameters investigated were time spent in the corners, time spent in the center, the velocity of the animal and the time spent immobile. Prior to entering the arena, the animals were kept in a smaller box which has dimensions similar to their home cage for 10 minutes to prevent any effect of novelty during the exploration in the main arena

Figure 10: Open field test setup. Image showing the arena settings and the corner and center zones for open field test. The areas marked as A, B, C and D are the corner zones while the area marked as E is the central zone

Mice tend to show a lesser proclivity to open areas which are brightly lit. If the animal is more anxious, it will result in lesser locomotive activity, and the animal will spend more

time at the corners of the arena rather than in the middle. Conversely, if the animal is less anxious, then it shows more expl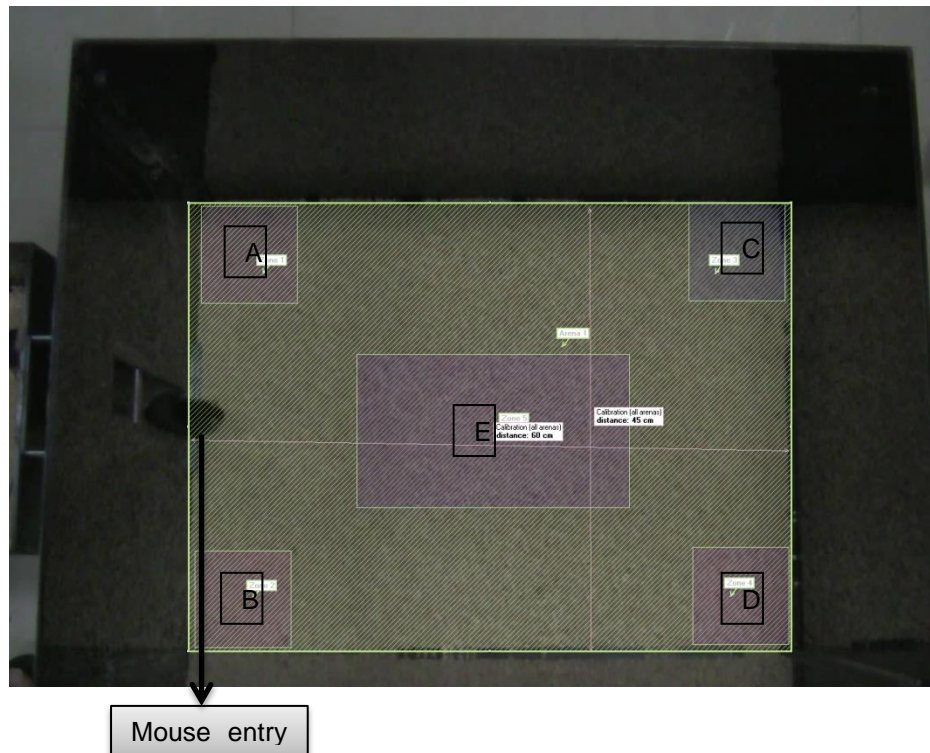oratory behavior, resulting in more locomotion activity and comparatively lesser time spent in the corners of the arena (Hall and Ballachey, 1932, Takahashi et al., 2006).

2.9 Pheromonal detection test

This test was done to check whether our injections have had any effects on the pheromone detection system of the animals. The vomeronasal organ is the primary center for pheromone detection in mammals. The neurons form the vomeronasal organ project to the accessory olfactory bulb (AOB)(Rodriguez and Boehm, 2008; Thorne and Amrein, 2003). The arena used was similar to that of the open field test. Soiled bedding containing urinary pheromones was taken from cages housing the female mice. (Bind et al., 2013). A petri dish of diameter 10 cm containing this bedding was kept in the exact center of the arena such that the dish was not visible and surrounded with fresh bedding. The time spent by the mice sniffing this zone was measured and compared across the three groups. Fresh bedding was used while animals from separate cages were tested.
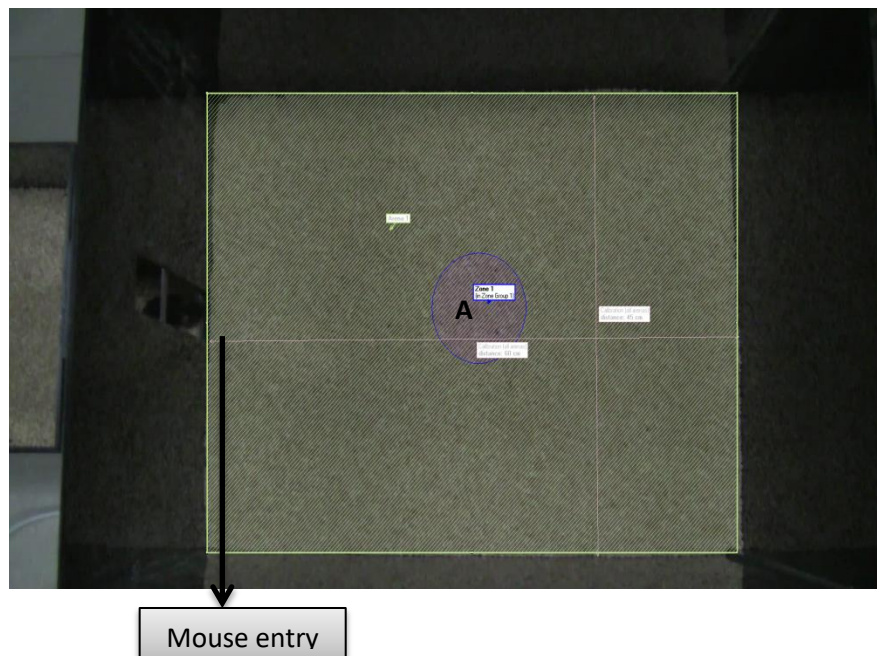
Figure 11: Pheromone detection test setup Image showing the arena settings and the female bedding zone for the pheromone detection task. The area marked as A has a petri plate containing bedding from a female cage

2.10 Buried food pellet test

The buried food pellet test is carried out to assess the ability of food-deprived mice to find out the location of the buried food pellet using odor cues emanating from the pellet (Machado et al., 2018). The animal was challenged to find a pellet which is buried under the bedding in the arena. The dimensions of the arena were same as that of the OFT and pheromone detection test (Figure 12). The test was carried over a time period of 4 days wherein the food pellet was buried below the surface for 3 days and for the 4th day a surface pellet was kept as a visual control. The latency to find the pellet by the mice is the main parameter that is observed in this test.

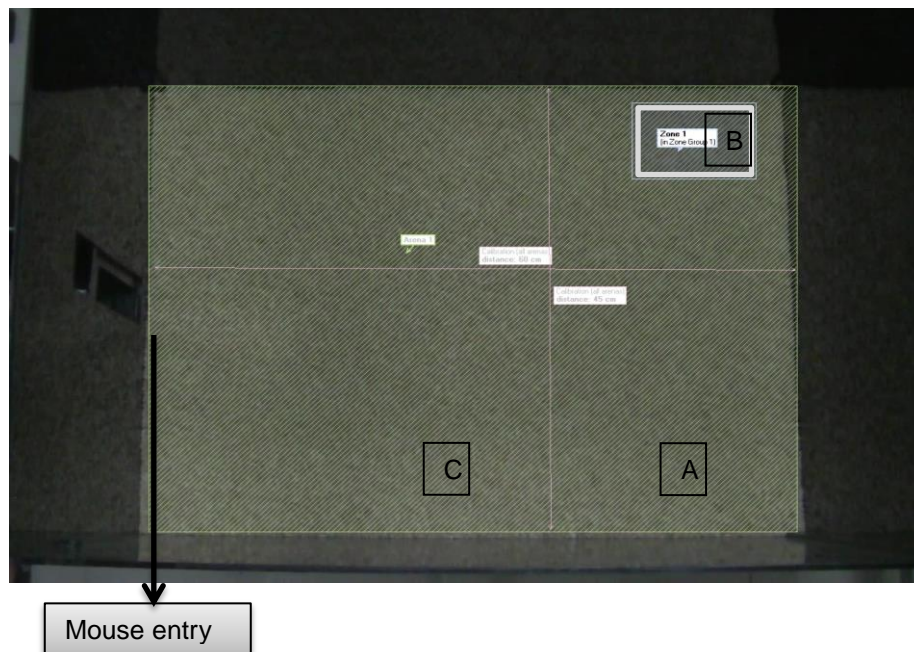Figure 12: Buried food pellettest setup. Image showing the arena settings and buried pellet zones for open field test. The areas marked as A, B and C are the zones where the pellet is buried for three different trials.

3. Results and Discussion

Olfactory deficits are symptom of many major neurodegenerative diseases including Parkinson's disease. Impairments of the olfactory system appear very early as compared to the classical motor symptoms of the disease, thus also called as prodromal symptoms of the disease (Doty, 2008). Foreign agents such as xenobiotics, toxins, bacteria, viruses, etc gain access to the olfactory bulb via the olfactory epithelium (OE) which can cause protein misfolding locally in the OE or OB . This may lead to a prion-like propagation of the misfolded protein to other parts of the brain (reviewed in (Rey et al., 2018a)). According to Braak's staging system of progression of sporadic PD, the Lewy body formation first takes place in the OB and the dorsal motor nucleus of the vagus nerve (Stage 1) (Braak et al., 2003). The pathology then spreads to the other regions of the brain in further Stages 2-6. These Stages indicate the development of pathology in different brain regions as the disease progresses.

We created a pre-clinical or prodromal model of PD in mice. As the OB is considered as one of the starting points for the spread of pathology of PD to the other brain regions, we stereotactically injected α-syn protein in the granule cell layer of the OB of wild type mice. Three different structural forms of the α-syn protein i.e. the protein in its native monomeric form and two abnormally aggregated forms, α-syn oligomers and α-syn fibrils were injected in the OB of three different groups of wild type mice. We wanted to investigate whether injecting structurally different forms of the protein may lead to differential development of the symptoms. The odor discrimination task was carried out at a time point of 2 weeks post injection while the rest of the behavioral tests were carried out at a time point of around 14 weeks post injection. The main finding of this thesis is that wild type mice which were stereotactically injected with α-syn oligomers in the granule cell layer of the olfactory bulb exhibited olfactory deficits, but their motor abilities remained unaffected.

3.1 Odor discrimination task

Two odor discrimination tasks were carried out to check the effect of stereotactic injection of the different structural forms of α-syn in the granule cell layer (GCL) of the animals. The three groups of mice were as follows:

Group 1: Mice injected with monomeric form of α-syn,

Group 2: Mice injected with oligomeric form of α-syn and

Group 3: Mice injected with fibrillar form of α-syn

Each group containing 9 animals were further divided into two sets of 4 and 5 animals. The rewarded (S+) and non-rewarded (S-) odors were swapped between these two sets.

First odor pair (table 1)

Odors used: **Binary Mixtures of 1-Heptanol (Hp): Nonanol (Nn)**	
Set 1	
Rewarded odor composition S(+)	1-Heptanol (Hp) : Nonanol (Nn) in 60:40 proportion
Non-rewarded odor composition S(-)	1-Heptanol (Hp) : Nonanol (Nn) in 40:60 proportion
Set 2	
Rewarded odor composition S(+)	Nonanol (Nn): 1-Heptanol (Hp) in 60:40 proportion
Non-rewarded odor composition S(-)	Nonanol (Nn): 1-Heptanol (Hp) in 40:60 proportion

Second odor pair (table 2)

Odors used : **Binary Mixtures of (S)-(+)- Octanol (+O) : (R)-(-)-Octanol (-O)**	
Set 1	
Rewarded odor composition S(+)	(S)-(+)- Octanol (+O) : (R)-(-)-Octanol (-O) in 60:40 proportion
Non-rewarded odor composition S(-)	(S)-(+)- Octanol (+O) : (R)-(-)-Octanol (-O) in in 40:60 proportion
Set 2	
Rewarded odor composition S(+)	(R)-(-)-Octanol (-O) : (S)-(+)- Octanol (+O) in 60:40 proportion
Non-rewarded odor composition S(-)	(R)-(-)-Octanol (-O) : (S)-(+)- Octanol (+O) in 40:60 proportion

3.1.1 Wild type mice injected with oligomeric form of α-synuclein showed olfactory deficits

The learning curves (Figure 13.A) and percentage accuracy graphs (Figure 13.B) for the three groups for Hp. vs. Nn. odor pair were plotted. The learning curves were plotted from the beginning of task 1 to the end of task 3 (1st trial to the 900th trial) . As seen from the curves, group 1 (monomer injected) animals started with slightly better accuracy as compared to group 2 (oligomer injected) and group 3 (fibril injected) animals. Monomer

injected animals started to learn at the end of task 1 (300 trials). The learning of oligomers-injected animals and fibrils-injected animals was around chance level by the end of task 1. After the completion of task 1, the learning pace across the three groups started to rise with monomers-injected mice showing the fastest learning pace followed by fibrils-injected mice. Oligomers-injected exhibited learning impairment, reaching the final average accuracy of around 80%. There was a significant difference in the percentage accuracies of the animals across the three groups across multiple data points on the learning curves as shown in Figure 13.A (Ordinary Two-way ANOVA, F-value = 2.801, p-value = 0.00041). The percentage accuracy (Figure 13.B) of monomers-injected animals for the final task (601-900 trials) was around 95%, that of oligomers-injected animals was just exceeding 80%, and that of fibrils-injected animals was around 90%. There was a significant difference observed between the percentage accuracies of monomers-injected animals vs. oligomers-injected animals and oligomers-injected animals vs. fibrils-injected animals (Ordinary One-way ANOVA, F-value = 22.94, p-value<0.0001).

The reaction times of wild type mice injected with the three different structural forms of α-syn were also calculated across the three groups for the final task (601 to 900 trials) and plotted as bar graphs. For the first odor pair, Hp. vs. Nn. (Figure13.C), monomers-injected and fibrils injected animals learnt to discriminate faster than the oligomers-injected animals. The reaction time values were not significantly different for monomers-injected animals vs. fibrils-injected animals. There was a significant difference between the reaction times of monomers-injected animals vs. oligomers-injected animals (300ms vs 500ms) and fibrils-injected animals vs. oligomers-injected animals (350ms vs 500ms) (Ordinary One-way ANOVA, F-value = 12.09, p-value=0.0002).
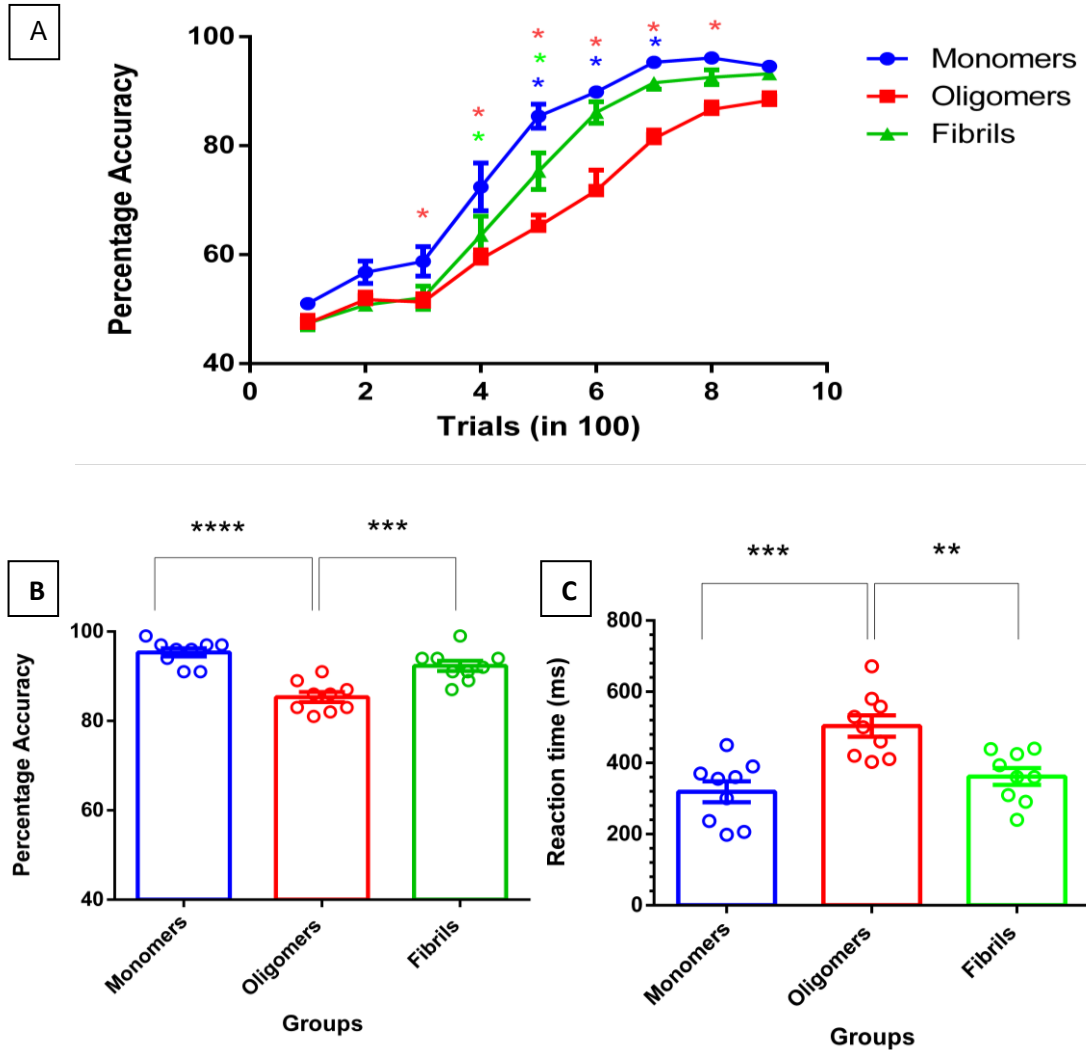
Figure 13. Hp. vs Nn. Odor discrimination task readouts. (A) Learning curves (Ordinary Two-way ANOVA, F-value = 2.801, p-value = 0.00041), (B) Percentage accuracies (mean ± SEM) (Ordinary One-way ANOVA, F-value = 22.94, p-value<0.0001) and (C) Reaction times (mean ± SEM) (Ordinary One-way ANOVA, F-value = 12.09, p-value=0.0002) of monomers-injected (blue), oligomers-injected (red) and fibrils-injected (green) animals for Hp. vs. Nn odor discrimination tasks.

The asterisks (Fig 13.B, 13.C) indicate a significant difference between percent accuracy and reaction times of group 1 vs. group 2 and group 2 vs. group 3.

A green asterisk Fig 13.A indicates a significant difference between group 1 vs. group 2 data points, blue asterisk indicates a significant difference between group 2 vs. group 3 data points and green asterisk indicates a significant difference between group 1 vs. group 3 data points.

The learning curve for the +O vs. -O odor pair is shown below in Figure 14.A. The curves for the three groups did not show any statistically significant difference over the three tasks (Ordinary Two-way ANOVA, F-value = 0.5727, p-value = 0.9022). The percentage accuracy in the third task of the second odor pair (Figure 14. B) was also similar across the three groups, reaching ~ 95% and no significant difference was observed between the accuracies of the three groups (Ordinary One-way ANOVA, F-value = 1.045, p-value= 0. 3671).

The reaction times of the mice across the three groups for the +O vs. -O odor discrimination task followed the same trend as that of the Hp. vs Nn. odor discrimination task. The reaction time for monomers-injected animals was slightly below 300 ms, while that of oligomers-injected animals was significantly higher at ~ 450 ms and that of fibrils-injected animals was significantly high than monomers-injected animals but significantly lower than oligomers-injected animals at just below 400 ms (Figure 14.C) (Ordinary One-way ANOVA, F-value = 19.42, p-value<0.0001). Interestingly, even though the oligomers-injected animals learnt to an average accuracy which was comparable to that of monomers-injected animals and fibrils-injected animals, they still took longer reaction times to discriminate between the second odor pair. This could be due to the dynamicity an *in vivo* system provides. One of the possible reasons is that the oligomer-injected animals learnt the procedural aspects of the paradigm during the first odor discrimination training. Alternatively, the protein aggregates may have traversed to interconnected brain regions from the site of their injections. However, we need to confirm this by carrying out immunohistochemistry of the oligomeric α-syn in the brain sections of these animals.
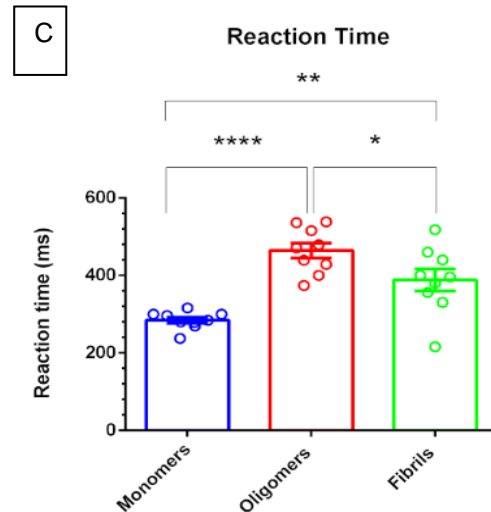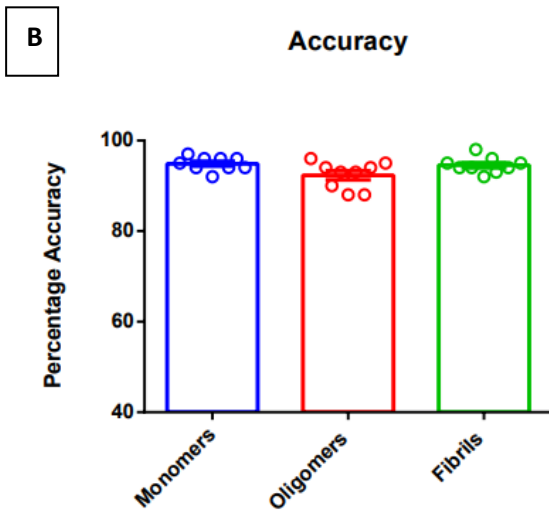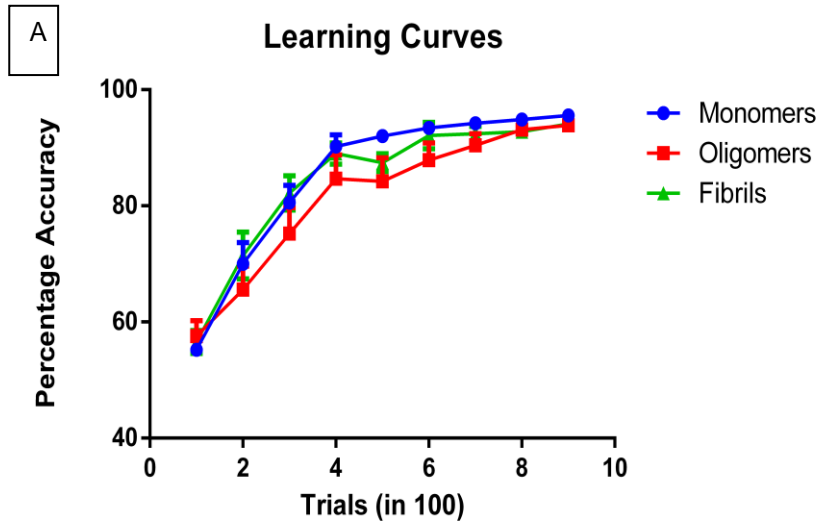
Figure 14. +O vs. -O. odor discrimination task readouts. (A) Learning curves (Ordinary Two-way ANOVA, F-value = 0.5727, p-value = P = 0.9022), (B) Percentage accuracies (mean ± SEM) (Ordinary One-way ANOVA, F-value = 1.045, p-value= 0.3671) and (C) Reaction times (mean ± SEM) (Ordinary One-way ANOVA, F-value = 19.42, p-value<0.0001) of monomers-injected (blue), oligomers-injected (red) and fibrils-injected (green) animals for +O vs -O odor discrimination tasks.

The asterisks (Fig 14.C) indicate a significant difference between reaction times of group 1 vs. group 2 and group 2 vs. group 3.

3.1.2 Behavioral deficits are not due to the differences in the motivation levels

To investigate if the motivation levels are accounting for the olfactory deficits we observed, we calculated different parameters defining the motivation of animals. For the first odor pair (Hp. vs. Nn.), the inter-trial interval (ITI) (Figure 15.A) for the final task across the three groups did not have any significant difference (Ordinary One-way ANOVA, F-value = 1.948, p-value=0.1644). Similar to the first odor pair, the inter-trial interval (ITI) for the second odor pair (+O vs. –O) (Figure 15.B) also did not show any significant difference over the final task for the three groups (Ordinary One-way ANOVA, F-value = 1.045, p-value=0.3671).

The lick percentage for the first odor pair (Hp. vs. Nn.) (Figure 15.C) was also statistically insignificant across the three groups (Ordinary One-way ANOVA, F-value = 0.1104, p-value=0.8959). The lick percentage (Figure 15.D) for second odor pair (+O vs. –O) was similar as well across the three groups for the final task and no significant difference was observed across them (Ordinary One-way ANOVA, F-value = 0.0404, p-value=0.9605).
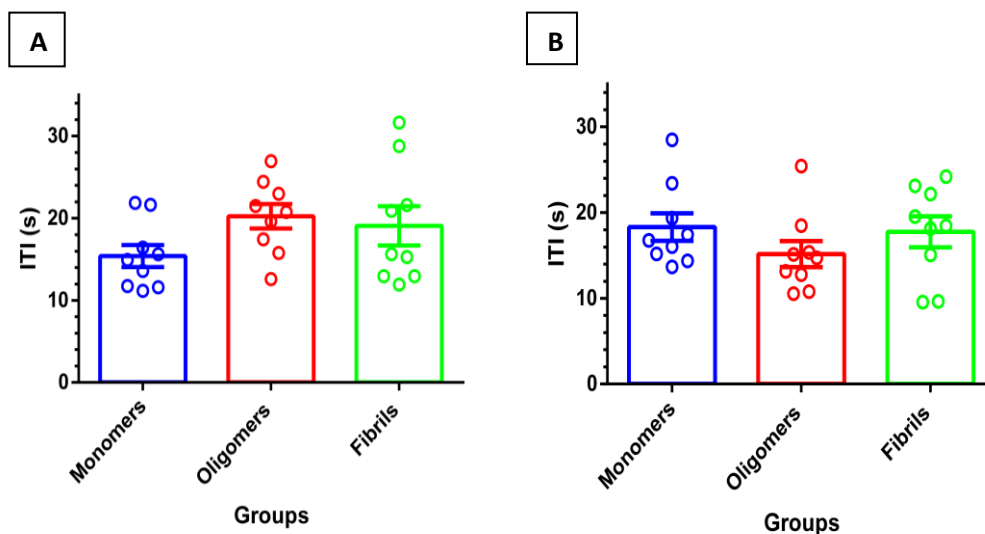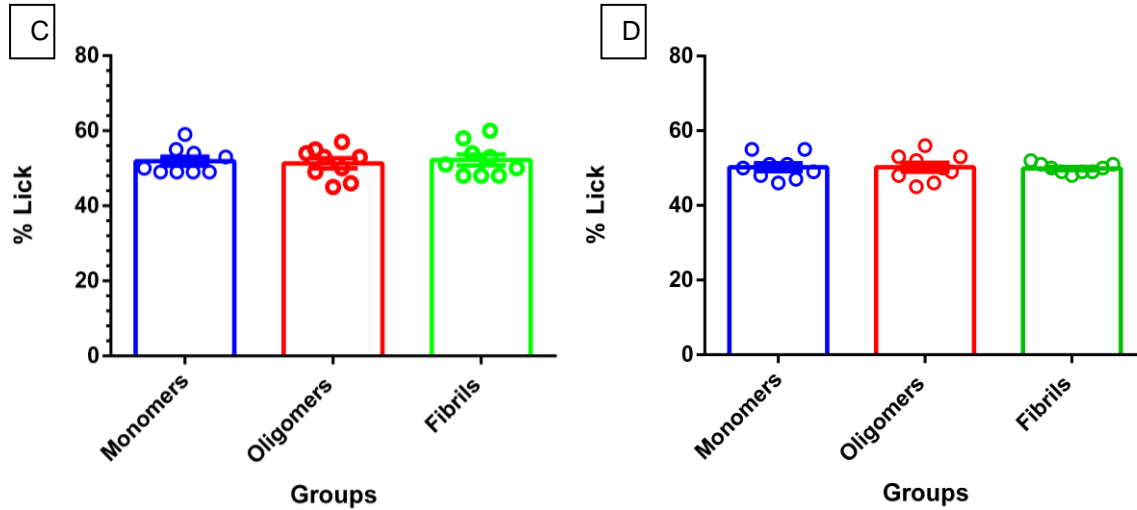
Figure 15: Motivation level readouts for both odor discrimination task .A) Inter-trial interval for Hp vs. Nn (mean ± SEM) (Ordinary One-way ANOVA, F-value = 1.948, p-value=0.1644) and B) +O vs. -O (Ordinary One-way ANOVA, F-value = 1.045, p-value=0.3671) and Percentage lick for (mean ± SEM) for C) Hp vs. Nn (mean ± SEM) (Ordinary One-way ANOVA, F-value = 0.1104, p-value=0.8959) and D) +O vs. -O (Ordinary One-way ANOVA, F-value = 0.0404, p-value=0.9605) of monomers-injected (blue), oligomers-injected (red) and fibrils-injected (green) animals in odor discrimination task.

Our findings about olfactory impairments in animals by intrabulbar delivery of oligomeric α-syn provided similar results compared to another study in which we delivered the aggregated forms of α-syn by intranasal infusion (see Appendix 1).

GCL specific delivery of α-syn aggregates brought about defects in olfactory discrimination and learning. These olfactory deficits could be due to the impaired functioning of granule cells inhibitory network. We are aware that spatio-temporal representations of odorants start forming at the level of activated glomeruli and are getting refined by the inhibitory circuits at the level of GL and GCL. These reciprocal synapses, thus, play an important role in odor discrimination. Our α-syn injections target

30-40 % of the entire granule cell population thus affecting the activity of GCs thereby modulating recurrent and lateral inhibition on the M/T cells. Rey et al., 2016 showed impaired odor detection and odor retention abilities but no deficits in odor discrimination abilities in animals by a unilateral non-specific delivery of human and mice α-syn pre-formed fibrils (PFFs) in the mouse OB. An advantage of our study over that of Rey et al., 2016, is that we have carried out a granule cell layer specific injections of the aggregated forms of α-syn. The odor discrimination abilities are largely modulated by the GCs of the OB. We have successfully demonstrated that our granule cell specific injections of α-syn oligomers show impaired reaction times with the phenotype appearing as early as 2 weeks post-injections. We did not observe deficits in the odor discrimination abilities in the fibrils-injected animals at a time point of 2 weeks post-injection but olfactory deficiencies were observed at 1 month post-injection. This finding is congruous with those reported in Rey et al., 2016 which state the onset of behavioral deficits starting from a 1 month post injection time point. More strikingly, in our experiments the oligomeric form of aggregates caused more severe impairments of olfactory functions as compared to the fibrillar form of α-syn. The electrophysiological basis of these behavioral deficits will be further investigated in detail.

3.2 All three groups of mice exhibit similar motor abilities

The vertical pole test was performed to check for any motor deficits caused due to the injection of the three structurally different forms of α-syn in the OB. The average time taken to make a completely downward turn of the snout (T turn) and the total time taken to descend the pole (T total) across three trials were measured and plotted as bar graphs. The average T turn (Fig 16.A) and the T total (Fig 16.B) across the three groups were comparable. There was no significant difference in the T turn (Ordinary One-way ANOVA, F-value = 0.2232, p-value= 0.8017) as well as T total (Ordinary One-way ANOVA, F-value = 0.6688, p-value= 0.5220) across the three groups of animals.
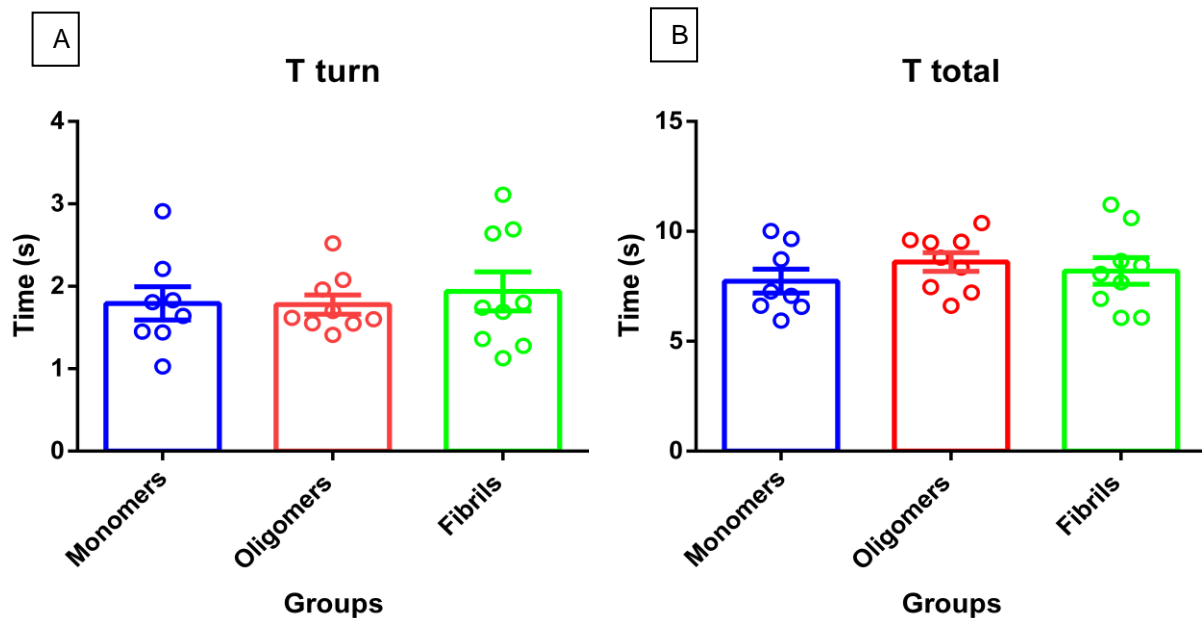
Figure 16: Vertical pole test readouts A) Time taken to turn (mean ± SEM) (Ordinary One-way ANOVA, F-value = 0.2232, p-value= 0.8017) and B) Total time taken to descend (mean ± SEM) (Ordinary One-way ANOVA, F-value = 0.6688, p-value= 0.5220) of monomers-injected (blue), oligomers-injected (red) and fibrils-injected (green) animals in a vertical pole test.

3.3 Anxiety levels and locomotive abilities were similar across the three groups

The results of the open field test indicated similar anxiety levels across all three groups of mice. The parameters that were looked at in the open field test were the time spent by the animal in the corners of the arena (T corner), the time spent in the center of the arena (T center), the average speed of the animal in the arena and the duration for which the animal remained immobile in the arena. The average time spent in the corners of the arena (Figure 17. A) had no significant difference across the three groups in the T corner measurements (Ordinary One-way ANOVA, F-value = 2.304, p-value= 0.1224). The time spent in the center of the arena (Figure 17. B) was significantly higher for monomers-injected animals when compared to oligomers-injected animals but for all

other comparisons, it was non-significant (Ordinary One-way ANOVA, F-value = 4.563, p-value= 0.0214). The average speed of the animal in the arena (Figure 17.C) was also non-significant across the three groups (Ordinary One-way ANOVA, F-value = 1.876, p-value = 0.1758). The total duration of time spent immobile by the animal (Figure 17.D) was also calculated and lacked any significant difference across the three groups (Ordinary One-way ANOVA, F-value = 0.1492, p-value = 2.069).
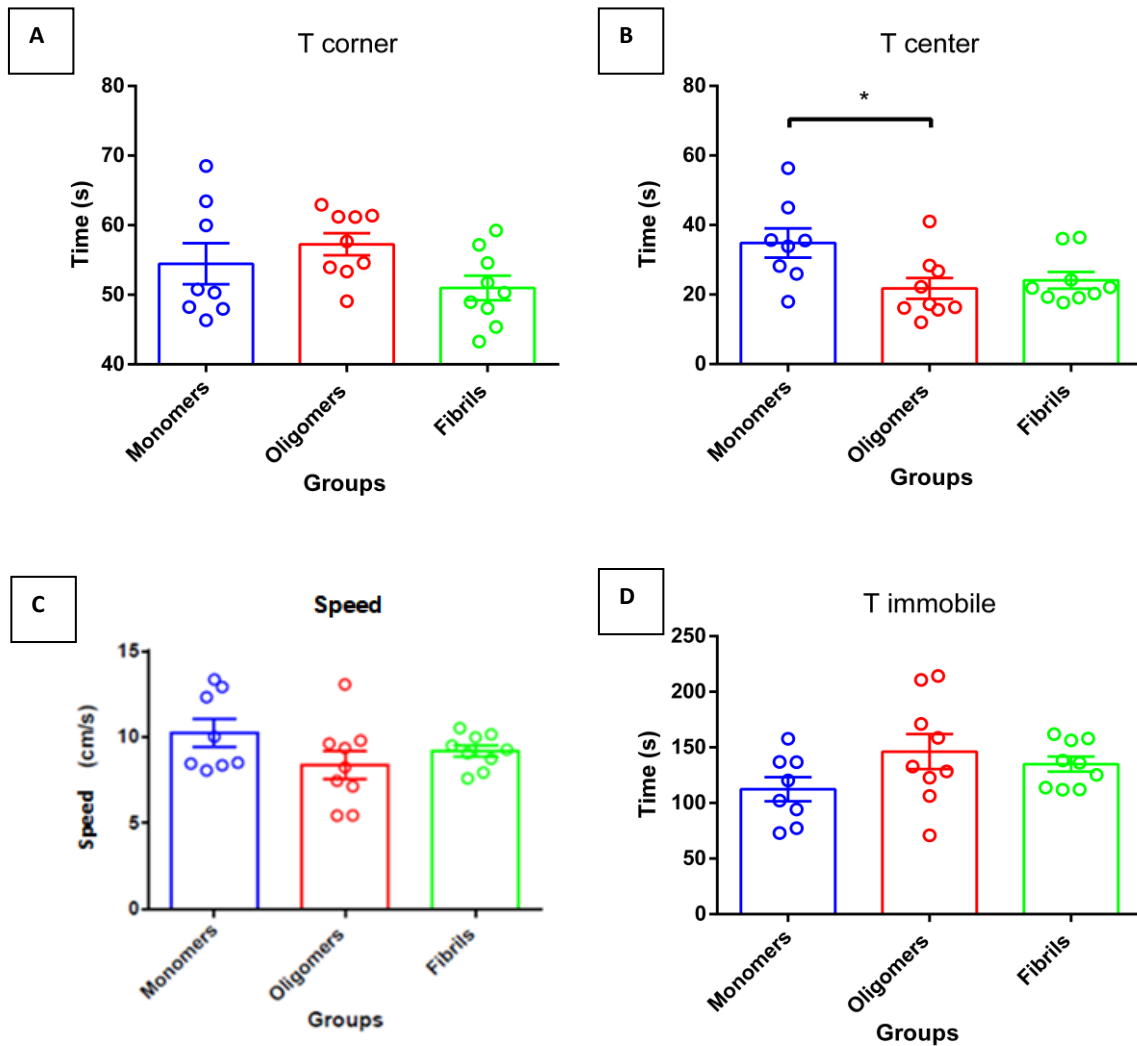
Figure 17: Open field test readouts: A) Average time spent in the corners (mean ± SEM) (Ordinary One-way ANOVA, F-value = 2.304, p-value= 0.1224), B) Time spent in the center (mean ± SEM) (Ordinary One-way ANOVA, F-value = 4.563, p-value= 0.0214), C) Average speed of animals (mean ± SEM) (Ordinary One-way ANOVA, F-value = 1.876, p-value= 0.1758), and D) time spent immobile (mean ± SEM) (Ordinary One-way ANOVA, F-value = 0.1492, p- value=2.069) by the animals across monomers-injected (blue), oligomers-injected (red) and fibrils-injected (green) in an open field test.

3.4 Pheromone detection abilities were similar across the three groups

The time spent by the mice in the zone containing bedding from female cages was compared across the three groups. There was no significant difference between any of the three groups, thus indicating that the pheromonal detection abilities were similar across the three groups (Figure 18) (Ordinary One-way ANOVA, F-value = 0.1911, p-value = 0.8273).
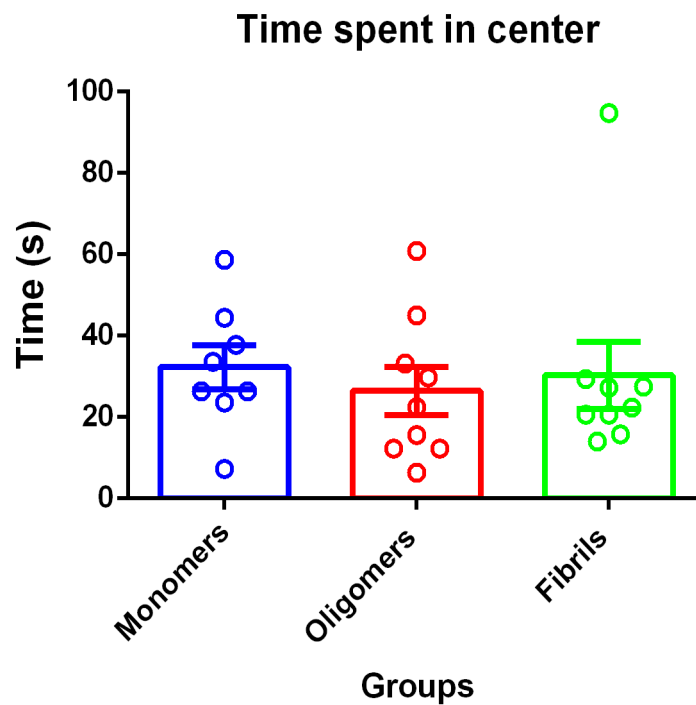

Time spent in center

Figure 18: Pheromone detection test readouts. Average time (mean ± SEM) (Ordinary One-way ANOVA, F-value = 0.1911, p-value = 0.8273) spent in the center by the animals across monomers-injected (blue), oligomers-injected (red) and fibrils-injected (green) in pheromone detection test.

3.5 Mice injected with oligomeric form of α-synuclein showed altered odor detection abilities

The time taken by the mice to find the buried food pellet was measured and compared across the three groups of animals. Average time taken over the course of three trials was plotted and compared across the three groups of animals. The results displayed higher latency to find the pellet in oligomers-injected group when compared to fibrils-injected group (Figure 19) (Ordinary One-way ANOVA, F-value = 4.804, p-value= 0.0181).
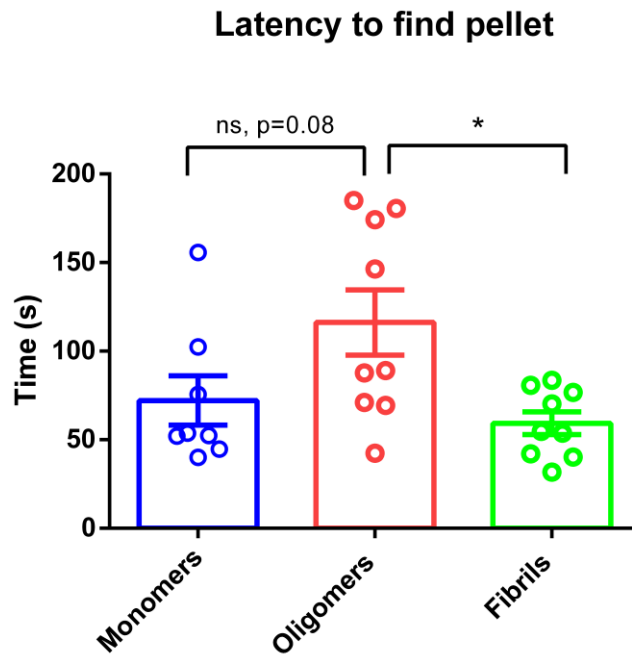
Latency to find pellet

Figure 19. Buried food pellet task readouts A) Time taken to find the pellet (Mean with SEM) (Ordinary One-way ANOVA, F-value = 4.804, p-value= 0.0181) for monomers-injected (blue), oligomers-injected (red) and fibrils-injected (green) animals in a buried food pellet task.

The findings of this thesis run in accordance with an earlier study carried out by Zhang et al., published in January 2019, reported that the deletion of dopaminergic neurons in the substantia nigra pars compacta (SNpc) region of the brain leads to impairments in neural activity in the olfactory bulb (Zhang et al., 2019). They demonstrated significant impairments in odor discrimination abilities and odor spatial memory in mice seven days post-injection with dopaminergic toxin 6-hydroxydopamine (6-OHDA) in the SNpc. However, the motor abilities which were checked through the rotarod test, remained unaffected in these mice.

Our studies were performed on wild-type C57BL6J male mice and no genetic manipulations were involved to create a PD model in these mice. We were able to successfully establish an early-onset PD model by intra-bulbar injections of α-syn at an age of 2 months. An advantage that our paradigm provides is that we can also establish a late-onset PD model by carrying injections at later adulthood (>6 months) in mice.

We plan to carry out immunohistochemical analysis for the presence and spread of abnormally aggregated α-syn from the site of injections to the interconnected brain regions across these three groups of animals. We want to investigate if the spread of these aggregates is varying across the three groups.

Another prospective study is investigating the action of artificially synthesized tryptophan-based compounds by injecting them in the same PD mouse models. These compounds have been shown to cause disassembly of the α-syn aggregates in *in vitro* experiments carried out in our lab. We plan to check whether there would be a recovery in the behavioral phenotype of the PD mice model, which we created upon the delivery of these compounds.

4. Appendix

4.1 Intranasal delivery of α-synuclein oligomers resulted in impaired olfactory reaction times

Three structurally different forms of α-syn protein were intranasally injected in wild type mice by another lab member, Niyoti Tembulkar. This is yet another proven strategy to create PD models which has shown to bring about maladaptive changes at the behavioral level (Gruden et al., 2014). She performed a Hp. vs. Nn. odor discrimination task for the three groups of animals and observed that the oligomers-injected group exhibited significantly higher reaction times after the injections as compared to the reaction time before injection (Figure 20).
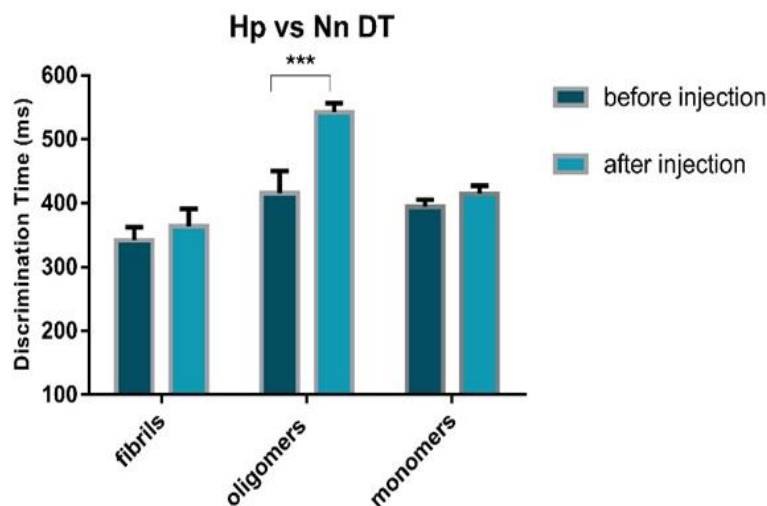

Figure 20. Reaction times for 1-Heptanol (Hp) vs Nonanol (Nn) odor discrimination task of intranasally injected wild type mice with three structurally different forms of injected α-synuclein before and after injection.

The asterisk indicate a significant difference between reaction times of wild type mice before and after intranasal injection of α-synuclein oligomers

5. References

Abraham, N.M., Spors, H., Carleton, A., Margrie, T.W., Kuner, T., and Schaefer, A.T. (2004). Maintaining accuracy at the expense of speed: Stimulus similarity defines odor discrimination time in mice. Neuron *44*, 865–876.

Abraham, N.M., Egger, V., Shimshek, D.R., Renden, R., Fukunaga, I., Sprengel, R., Seeburg, P.H., Klugmann, M., Margrie, T.W., Schaefer, A.T., et al. (2010). Synaptic Inhibition in the Olfactory Bulb Accelerates Odor Discrimination in Mice. Neuron *65*, 399–411.

Adler, C.H. (2011). Premotor Symptoms and Early Diagnosis of Parkinson's Disease. Int. J. Neurosci. *121*, 3–8.

Angot, E., Steiner, J.A., Lema Tomé, C.M., Ekström, P., Mattsson, B., Björklund, A., and Brundin, P. (2012). Alpha-synuclein cell-to-cell transfer and seeding in grafted dopaminergic neurons in vivo. PLoS One *7*, e39465.

Bhalla, U.S., and Bower, J.M. (1993). Exploring parameter space in detailed single neuron models: simulations of the mitral and granule cells of the olfactory bulb. J. Neurophysiol. *69*, 1948–1965.

Bind, R.H., Minney, S.M., Rosenfeld, S., and Hallock, R.M. (2013). The Role of Pheromonal Responses in Rodent Behavior : Future Directions for the Development of Laboratory Protocols. *52*.

Bodyak, N., and Slotnick, B. (1999). Performance of mice in an automated olfactometer: odor detection, discrimination and odor memory. Chem. Senses *24*, 637–645.

Braak, H., Del, K., Rüb, U., Vos, R.A.I. De, Jansen, E.N.H., and Braak, E. (2003). Braak H, 2003.pdf. *24*, 197–211.

Buck, L., and Axel, R. (1991). A novel multigene family may encode odorant receptors: a molecular basis for odor recognition. Cell *65*, 175–187.

Danzer, K.M., Krebs, S.K., Wolff, M., Birk, G., and Hengerer, B. (2009). Seeding induced by α-synuclein oligomers provides evidence for spreading of α-synuclein pathology. J. Neurochem. *111*, 192–203.

Dehay, B., Bourdenx, M., Gorry, P., Przedborski, S., Vila, M., Hunot, S., Singleton, A., Olanow, C.W., Merchant, K.M., Bezard, E., et al. (2015). Targeting α-synuclein for treatment of Parkinson's disease: mechanistic and therapeutic considerations. Lancet. Neurol. *14*, 855–866.

Diao, J., Burré, J., Vivona, S., Cipriano, D.J., Sharma, M., Kyoung, M., Südhof, T.C., and Brunger, A.T. (2013). Native α-synuclein induces clustering of synaptic-vesicle mimics via binding to phospholipids and synaptobrevin-2/VAMP2. Elife *2*, e00592.

Doty, R.L. (2008). The olfactory vector hypothesis of neurodegenerative disease: Is it viable? Ann. Neurol. *63*, 7–15.

Emamzadeh, F.N. (2016). Alpha-synuclein structure, functions, and interactions. J. Res. Med. Sci. *21*, 29.

Fink, A.L. (2006). The Aggregation and Fibrillation of α-Synuclein.

Flagmeier, P., Meisl, G., Vendruscolo, M., Knowles, T.P.J., Dobson, C.M., Buell, A.K., and Galvagnion, C. (2016). Mutations associated with familial Parkinson's disease alter the initiation and amplification steps of α-synuclein aggregation. Proc. Natl. Acad. Sci. U. S. A. *113*, 10328–10333.

Gruden, M.A., Davydova, T. V., Narkevich, V.B., Fomina, V.G., Wang, C., Kudrin, V.S., Morozova-Roche, L.A., and Sewell, R.D.E. (2014). Intranasal administration of alpha-synuclein aggregates: a Parkinson's disease model with behavioral and neurochemical correlates. Behav. Brain Res. *263*, 158–168.

Heemels, M.-T. (2016). Neurodegenerative diseases. Nature *539*, 179–179.

Hobson, D.E. (2012). Asymmetry in parkinsonism, spreading pathogens and the nose. Parkinsonism Relat. Disord. *18*, 1–9.

Hüttenbrink, K.-B., Hummel, T., Berg, D., Gasser, T., and Hähner, A. (2013). Olfactory dysfunction: common in later life and early warning of neurodegenerative disease. Dtsch. Arztebl. Int. *110*, 1–7, e1.

Isaacson, J.S., and Strowbridge, B.W. (1998). Olfactory reciprocal synapses: dendritic signaling in the CNS. Neuron *20*, 749–761.

Johnson, B.A., Ong, J., and Leon, M. (2010). Glomerular activity patterns evoked by natural

odor objects in the rat olfactory bulb are related to patterns evoked by major odorant components. J. Comp. Neurol. *518*, 1542–1555.

Jucker, M., and Walker, L.C. (2013). Self-propagation of pathogenic protein aggregates in neurodegenerative diseases. Nature *501*, 45–51.

Kiyokage, E., Pan, Y.-Z., Shao, Z., Kobayashi, K., Szabo, G., Yanagawa, Y., Obata, K., Okano, H., Toida, K., Puche, A.C., et al. (2010). Molecular identity of periglomerular and short axon cells. J. Neurosci. *30*, 1185–1196.

Kordower, J.H., Dodiya, H.B., Kordower, A.M., Terpstra, B., Paumier, K., Madhavan, L., Sortwell, C., Steece-Collier, K., and Collier, T.J. (2011). Transfer of host-derived α synuclein to grafted dopaminergic neurons in rat. Neurobiol. Dis. *43*, 552–557.

Lee, V.M.-Y., and Trojanowski, J.Q. (2006). Mechanisms of Parkinson's Disease Linked to Pathological α-Synuclein: New Targets for Drug Discovery. Neuron *52*, 33–38.

Lledo, P.-M., Gheusi, G., and Vincent, J.-D. (2005). Information Processing in the Mammalian Olfactory System. Physiol. Rev. *85*, 281–317.

Luk, K.C., Song, C., O'Brien, P., Stieber, A., Branch, J.R., Brunden, K.R., Trojanowski, J.Q., and Lee, V.M.-Y. (2009). Exogenous alpha-synuclein fibrils seed the formation of Lewy body-like intracellular inclusions in cultured cells. Proc. Natl. Acad. Sci. U. S. A. *106*, 20051–20056.

Machado, C.F., Reis-Silva, T.M., Lyra, C.S., Felicio, L.F., and Malnic, B. (2018). Buried Food-seeking Test for the Assessment of Olfactory Detection in Mice. Bio-Protocol *8*, e2897.

Malnic, B., Hirono, J., Sato, T., and Buck, L.B. (1999). Combinatorial Receptor Codes for Odors. Cell *96*, 713–723.

Margrie, T.W., Sakmann, B., and Urban, N.N. (2001). Action potential propagation in mitral cell lateral dendrites is decremental and controls recurrent and lateral inhibition in the mammalian olfactory bulb. Proc. Natl. Acad. Sci. *98*, 319–324.

Meissner, W.G., Frasier, M., Gasser, T., Goetz, C.G., Lozano, A., Piccini, P., Obeso, J.A., Rascol, O., Schapira, A., Voon, V., et al. (2011). Priorities in Parkinson's disease research. Nat. Rev. Drug Discov. *10*, 377–393.

Mombaerts, P. (2001). How smell develops. Nat. Neurosci. *4*, 1192–1198.

Mombaerts, P., Wang, F., Dulac, C., Chao, S.K., Nemes, A., Mendelsohn, M., Edmondson, J., and Axel, R. (1996). Visualizing an olfactory sensory map. Cell *87*, 675–686.

Nagayama, S., Homma, R., and Imamura, F. (2014). Neuronal organization of olfactory bulb circuits. Front. Neural Circuits *8*, 98.

Ogawa, N., Hirose, Y., Ohara, S., Ono, T., and Watanabe, Y. (1985). A simple quantitative bradykinesia test in MPTP-treated mice. Res. Commun. Chem. Pathol. Pharmacol. *50*, 435–441.

Ponsen, M.M., Stoffers, D., Booij, J., van Eck-Smit, B.L.F., Wolters, E.C., and Berendse, H.W. (2004). Idiopathic hyposmia as a preclinical sign of Parkinson's disease. Ann. Neurol. *56*, 173–181.

Prediger, R.D.S., Matheus, F.C., Schwarzbold, M.L., Lima, M.M.S., and Vital, M.A.B.F. (2012). Anxiety in Parkinson's disease: A critical review of experimental and clinical studies. Neuropharmacology *62*, 115–124.

Price, J.L., and Powell, T.P.S. (1970). THE MORPHOLOGY OF THE GRANULE CELLS OF THE OLFACTORY BULB.

Prusiner, S.B. (2001). Neurodegenerative Diseases and Prions. N. Engl. J. Med. *344*, 1516–1526.

Ressler, K.J., Sullivan, S.L., and Buck, L.B. (1993). A zonal organization of odorant receptor gene expression in the olfactory epithelium. Cell *73*, 597–609.

Rey, N.L., Petit, G.H., Bousset, L., Melki, R., and Brundin, P. (2013). Transfer of human α-synuclein from the olfactory bulb to interconnected brain regions in mice. Acta Neuropathol. *126*, 555–573.

Rey, N.L., Lee, V.M.-Y., Madaj, Z., Brundin, P., Steiner, J.A., Luk, K.C., Trojanowski, J.Q., and Maroof, N. (2016). Widespread transneuronal propagation of α-synucleinopathy triggered in olfactory bulb mimics prodromal Parkinson's disease. J. Exp. Med. *213*, 1759–1778.

Rey, N.L., Wesson, D.W., and Brundin, P. (2018a). The olfactory bulb as the entry site for prion-like propagation in neurodegenerative diseases. Neurobiol. Dis. *109*, 226–248.

Rey, N.L., George, S., Steiner, J.A., Madaj, Z., Luk, K.C., Trojanowski, J.Q., Lee, V.M.-Y., and

Brundin, P. (2018b). Spread of aggregates after olfactory bulb injection of α-synuclein fibrils is associated with early neuronal loss and is reduced long term. Acta Neuropathol. *135*, 65–83.

Rodriguez, I., and Boehm, U. (2008). Pheromone Sensing in Mice. pp. 139–185.

Ross, G.W., Petrovitch, H., Abbott, R.D., Tanner, C.M., Popper, J., Masaki, K., Launer, L., and White, L.R. (2008). Association of olfactory dysfunction with risk for future Parkinson's disease. Ann. Neurol. *63*, 167–173.

Sengoku, R., Saito, Y., Ikemura, M., Hatsuta, H., Sakiyama, Y., Kanemaru, K., Arai, T., Sawabe, M., Tanaka, N., Mochizuki, H., et al. (2008). Incidence and Extent of Lewy Body-Related α-Synucleinopathy in Aging Human Olfactory Bulb. J. Neuropathol. Exp. Neurol. *67*, 1072–1083.

Shepherd, G.M. (2004). The Synaptic Organization of the Brain (Oxford University Press).

Shepherd, G.M., Chen, W.R., Willhite, D., Migliore, M., and Greer, C.A. (2007). The olfactory granule cell: From classical enigma to central role in olfactory processing. Brain Res. Rev. *55*, 373–382.

Singleton, A., Gwinn-Hardy, K., Sharabi, Y., Li, S., Holmes, C., Dendi, R., Hardy, J., Singleton, A., Crawley, A., and Goldstein, D.S. (2004). Association between cardiac denervation and parkinsonism caused by α-synuclein gene triplication. Brain *127*, 768–772.

Singleton, A.B., Farrer, M., Johnson, J., Singleton, A., Hague, S., Kachergus, J., Hulihan, M., Peuralinna, T., Dutra, A., Nussbaum, R., et al. (2003). α-Synuclein Locus Triplication Causes Parkinson's Disease. Science (80-.). *302*, 841.

Stefanis, L. (2012). α-Synuclein in Parkinson's disease. Cold Spring Harb. Perspect. Med. *2*, a009399.

Takahashi, A., Kato, K., Makino, J., Shiroishi, T., and Koide, T. (2006). Multivariate Analysis of Temporal Descriptions of Open-field Behavior in Wild-derived Mouse Strains. Behav. Genet. *36*, 763–774.

Thorne, N., and Amrein, H. (2003). Vomeronasal Organ: Pheromone Recognition with a Twist. Curr. Biol. *13*, R220–R222.

Uversky, V.N., Gillespie, J.R., and Fink, A.L. (2000). Why are ?natively unfolded? proteins

unstructured under physiologic conditions? Proteins Struct. Funct. Genet. *41*, 415–427.

Wakabayashi, K., Tanji, K., Mori, F., and Takahashi, H. (2007). The Lewy body in Parkinson's disease: molecules implicated in the formation and degradation of alpha-synuclein aggregates. Neuropathology *27*, 494–506.

Welsh, M.D. (2001). Measurement of quality of life in neurodegenerative disorders. Curr. Neurol. Neurosci. Rep. *1*, 346–349.

Wood, S.J., Wypych, J., Steavenson, S., Louis, J.C., Citron, M., and Biere, A.L. (1999). alpha-synuclein fibrillogenesis is nucleation-dependent. Implications for the pathogenesis of Parkinson's disease. J. Biol. Chem. *274*, 19509–19512.

Zhang, W., Sun, C., Shao, Y., Zhou, Z., Hou, Y., and Li, A. (2019). Partial depletion of dopaminergic neurons in the substantia nigra impairs olfaction and alters neural activity in the olfactory bulb. Sci. Rep. *9*, 254.